Pramāṇa – J. Phys., Vol. 27, Nos 1 & 2, July & August 1986, pp. 233–266.

Double-diffusive magnetoconvection

N RUDRAIAH

UGC-DSA Centre in Fluid Mechanics, Department of Mathematics, Central College, Bangalore University, Bangalore 560 001

Abstract. This review deals principally with the interaction between double-diffusive convection and an externally imposed vertical magnetic field in a Boussinesq fluid. Both linear and nonlinear (two and three-dimensional) theories have been discussed. Double-diffusive magnetoconvection is shown to exhibit a rich variety of dynamical behaviour unimaginable in a single component system and serves as a guide to the behaviour of all triple-diffusive systems. Finally, the effects of cross-diffusion, rotation and chemical reaction on double-diffusive magnetoconvection and pattern selection have been briefly touched upon.

Keywords. Double-diffusive convection; vertical magnetic field; Boussinesq fluid; cross-diffusion; pattern selection.

PACS No. 47·25

1. Introduction

1.1 *Scope*

Solar surface phenomena and the cosmical magnetic fields are generally associated with turbulent motion, which may be driven by multicomponent convection. Late-type stars like the sun have deep outer convective zones, where, in addition to the thermal and compositional gradients, there exist gradients in magnetic field and/or rotation. Multidiffusion effects may be expected as a result. The phenomena of overstability, subcritical over-turning instability and fingering all have their counterparts in the presence of gradients in angular momentum and magnetic field strength. The mixing effect of these instabilities on the chemical composition of the star has important consequences in our understanding of stellar convection.

The instabilities can occur either in the form of salt-finger or diffusive interfaces (Turner 1979; Griffiths and Ruddick 1980, Huppert and Turner 1981, Rudraiah and Shivakumara 1984, 1986a, b) depending on the values of the physical parameters. The key parameters appearing in the equations are

$\tau_1 = \kappa_s/\kappa$, the ratio of mass diffusivity κ_s to the thermal diffusivity κ, the ratio of
$\tau_2 = \nu_m/\kappa$, magnetic diffusivity ν_m to κ,
$\sigma = \nu/\kappa$, the ratio of kinematic viscosity ν to κ, which is the Prandtl number,

The author felicitates Prof. D S Kothari on his eightieth birthday and dedicates this paper to him on this occasion.

$R_T = \dfrac{\alpha_t g \Delta T d^3}{\nu\kappa}$ the Rayleigh number which represents the balance of energy released by buoyancy force and the energy dissipation by viscous and thermal effects,

$R_s = \dfrac{\alpha_s g \Delta S d^3}{\nu\kappa}$, the solute analog of R_T,

$Q = \dfrac{\mu H_0^2 d^2}{\rho_m \nu \nu_m}$, is the Chandrasekhar number which represents the measure of Lorentz force to viscous force,

where d is the depth of the fluid layer, ΔT and ΔS are respectively the temperature and concentration differences between the boundaries and ρ_m is the density at the ambient temperature.

In astrophysical context τ_2 is less than unity (see table 1) of order 0·6 (owing to the radiative heat transport) and in the laboratory experiments or in the earth's core it is greater than unity and τ_1 is always less than unity. The most significant double-diffusive magnetoconvection phenomena occur, in general, under conditions that are barely achievable in laboratory systems, notably when τ_2 and the magnetic Reynolds number R_m (which equals $\alpha_t g \Delta T d^3/\nu\nu_m$, where we have used the characteristic velocity $U = \alpha_t g \Delta T d^2/\nu$ because the motion is mainly induced by buoyancy force) is so high that the field is substantially distorted by the motion and the magnetic flux is swept into the regions of converging flow in a convecting layer. However, when τ_2 is small (advection competes with diffusion of magnetic flux) a whole range of new novel phenomena (explained in §1.2) arise. It is with the basic processes that underlie these novel phenomena that the study of the present review is largely concerned.

1.2 *The basic principles and unusual phenomena of double-diffusive magnetoconvection*

Copious literature concerning magnetoconvection in a single component system is now available (see Chandrasekhar 1961 for linear theory; Busse 1975; Peckover and Weiss 1978; Rudraiah 1981; Weiss 1981; Proctor and Weiss 1982 and Rudraiah *et al* 1985a, b for nonlinear theory). The study of convection in a two and multicomponent fluid layer where two scalar fields (such as heat and salinity concentration) affect the density distribution, is comparatively new and has recently drawn the attention of astrophysicists, geophysicists, oceanographers, engineers and a host of others (see Baines and Gill 1969; Turner 1974, 1979, 1981, Griffiths 1979a, b, c; Huppert and Turner 1981; Chen and Johnson 1984). Their study, both theoretical and experimental, has stimulated

Table 1. Some typical values of the quantities appearing in the dimensionless parameters.

	Earth	Sun
H_0 (Henry)	10^4	10^5
ρ_m (kg m^{-3})	10^4	10^3
μ (H m^{-1})	10^{-6}	10^{-6}
d (m)	10^6	10^8
ν (m^2 sec^{-1})	4×10^{-6}	10^5
κ (m^2 sec^{-1})	10^{-5}	$0{\cdot}1 \times 10^4$
ν_m (m^2 sec^{-1})	$0{\cdot}33 \times 10^4$	$0{\cdot}59 \times 10^2$

widespread interest to extend this concept to other fields. Therefore, much work has also been done on double-diffusive convection in a porous medium because of its natural occurrence and its applications in geophysics particularly in understanding the groundwater pollution and heat lost to the ground below unlined solar ponds (see Nield 1968; Wankat and Schowalter 1970; Taunton *et al* 1972; Tyvand 1980; Griffiths 1981; Rudraiah *et al* 1982a, b).

Most practical problems, be it astrophysical or geophysical, relate in some way or the other to problems concerning the external constraints like rotation and/or magnetic field operative on double-diffusive systems. In spite of its natural importance, much work has not been done in this direction. Pearlstein (1982) was the first to study, in detail, the effect of the Coriolis force on the double-diffusive convection and has shown that the effect of rotation and bottom-heavy solute gradient renders the system unstable under certain conditions. He has given the physical explanation based on the frequency of oscillations for this unusual phenomena. Recently, Rudraiah *et al* (1986a) have also shown the same unusual effect of the Coriolis force on the double-diffusive convection in a sparsely-packed porous medium and a different physical explanation than that of Pearlstein (1981) was given based on the phase-shift of dependent variables.

The external constraint of magnetic field on double-diffusive convection has not been given much attention. Lortz (1965) was the first to study the effect of magnetic field on double-diffusive convection. His object was to clarify some of the mathematical aspects of the so-called relative stability criterion of Malkus and Veronis (1958) but his analysis is silent about the detailed study of stability analysis. In view of this, recently Rudraiah and Shivakumara (1984, 1986a, b) and Shivakumara (1985) have investigated both linear and nonlinear theory of this problem in detail. They have shown that the magnetic field, under certain conditions makes the system unstable. They have also investigated the effect of magnetic field on the physically preferred cell pattern.

In this review we shall be concerned with the more restricted problem of double-diffusive convection in a Boussinesq electrically conducting fluid in the presence of an imposed vertical magnetic field, called double-diffusive magnetoconvection. The following are the main requirements for the occurrence of double-diffusive magnetoconvection:

(i) the fluid should be electrically conducting and must have atleast two components with different molecular diffusivities,

(ii) these components must make opposing contributions to the vertical density gradient,

(iii) magnetic diffusivity must act as a third diffusing component.

When the density gradient of more than one diffusing property is important a whole range of new phenomena can arise, and intuition that we have gained from the study of free convection of a single component fluid can be misleading, for example:

(i) In a single component fluid we know that when density decreases with height, the system is stable, whereas in a two-component system this is not always true. Even the decrease in density with height makes the system unstable.

(ii) Diffusion is generally a stabilizing factor in a single-component fluid. But in the case of two-component system it can act to release the potential energy in the component that is heaviest at the top and make the system unstable.

The physical reason for the occurrence of the above two interesting phenomena is clearly explained in the experiments of Stommel *et al* (1956) (see also the book by Turner 1979 for details).

(iii) In a single component fluid the effect of external constraint of rotation or magnetic field is to suppress convection. In a two-component system, it may augment or suppress convection under certain conditions. It is interesting to know how the otherwise stabilizing factors destabilize the system in two-component systems.

In addition to these three, recently Rudraiah and Shivakumara (1984) and Shivakumara *et al* (1985) have observed the following unusual phenomena in the presence of a magnetic field:

(iv) When a third property with a different diffusivity (say magnetic diffusivity) is added to the fluid, interesting things unimaginable in a two-component system, arise about the nature of interface. For example, the addition of a more slowly diffusing property to the bottom layer of a system that would otherwise have produced a 'finger' interface could cause a 'diffusive' interface. Similarly, addition of the same property to the top layer of another system may change the resulting interface from a 'diffusive' to a 'finger' kind.

In this review we shall be concerned with providing a theoretical model to explain these unusual phenomena. We deal with a more general system in the sense that the two components may be sucrose and sugar or may be a temperature and any solute in addition to magnetic diffusion. The problem of double-diffusive magnetoconvection is called thermohaline magnetoconvection when the two diffusive mechanisms are thermal and solute. Our review is mainly concerned with the thermohaline magnetoconvection. We shall discuss at some length the development of both linear and nonlinear thermohaline magnetoconvection with particular emphasis on the transition from time-dependent to steady finite amplitude thermohaline magnetoconvection.

Since the thermohaline convection in an ordinary fluid has been extensively discussed by many authors (see Turner 1974; Huppert and Turner 1981), this review is slanted towards the more recent development of thermohaline magnetoconvection in bifurcation theory and in the application of power integral and truncated representation techniques (which are asymptotic techniques). These techniques have made it possible to describe the development of finite amplitude behaviour in the neighbourhood of bifurcations from the static conducting state. Though we have a complete understanding of the nonlinear magnetoconvection in a single-component system due to the availability of larger and faster computers, the study of double-diffusive magnetoconvection is still in its infant stage. The available analytical and numerical techniques may be used to elucidate the complex nonlinear behaviour of double-diffusive magnetoconvection, which is among the best examples of triple-diffusive convection where the magnetic field acts as a third diffusing component. In this review we shall attempt to provide a description of double-diffusive magnetoconvection in two and three-dimensional geometries using analytical techniques.

The plan of the review is as follows. In §2, we derive the equations that govern Boussinesq double-diffusive magnetoconvection and discuss the boundary conditions and the equations for two-dimensional motion. Section 3 is devoted to the study of linear stability problem in detail. The two-dimensional finite amplitude double-diffusive magnetoconvection is discussed in §4 using truncated model system, considering both steady and unsteady cases. In §§5 to 7 we have studied the finite amplitude steady double-diffusive magnetoconvection in two- and three-dimensional

geometries using perturbation method. In the last section we briefly review the extension of the analytical methods to include cross-diffusion, chemical reaction and rotational effects.

2. Boussinesq double-diffusive magnetoconvection

2.1 *The governing equations*

Consider a horizontally stratified conducting Boussinesq binary fluid of depth d subjected to uniform heating from below and cooling from above on which the buoyancy force due to gravity, and the magnetic field act in the vertical direction. The temperature and solute are given by $\tilde{T} = T_m$, $\tilde{S} = S_m$ at $z = 0$ and $(T_m - \Delta T)$ and $(S_m - \Delta S)$ at $z = d$. We break up the temperature and solute into two parts such that $\tilde{T} = T_m - \Delta T z/d + T(x, y, z, t)$ and $\tilde{S} = S_m - \Delta S z/d + S(x, y, z, t)$ where the first two terms represent the conduction state and the last term is the convective state. We introduce a Cartesian co-ordinate system with the z-axis pointing vertically upwards. For convection in a Boussinesq fluid the velocity $\mathbf{q}$, the magnetic field $\mathbf{H}$, the temperature T, the concentration S, the pressure P and the density ρ satisfy the following dimensionless equations:

$$\frac{1}{\sigma}\left\{\frac{\partial \mathbf{q}}{\partial t} + (\mathbf{q}\cdot\nabla)\mathbf{q}\right\} = -\nabla P + Q\tau_2(\mathbf{H}\cdot\nabla)\mathbf{H} + (T - S)\hat{k} + \nabla^2\mathbf{q}, \tag{1}$$

$$\left(\frac{\partial}{\partial t} - \nabla^2\right)T + (\mathbf{q}\cdot\nabla)T = R_T\mathbf{q}\cdot\hat{k}, \tag{2}$$

$$\left(\frac{\partial}{\partial t} - \tau_1\nabla^2\right)S + (\mathbf{q}\cdot\nabla)S = R_S\mathbf{q}\cdot\hat{k}, \tag{3}$$

$$\left(\frac{\partial}{\partial t} - \tau_2\nabla^2\right)\mathbf{H} = \nabla\times(\mathbf{q}\times\mathbf{H}), \tag{4}$$

with $\nabla\cdot\mathbf{q} = \nabla\cdot\mathbf{H} = 0$ and $\rho = \rho_m\{1 - \alpha_t(\tilde{T} - T_m) + \alpha_s(\tilde{S} - S_m)\}$ where we have scaled length with d, time with d^2/κ, velocity with κ/d, magnetic field with H_0, temperature with $\nu\kappa/\alpha_t g d^3$ and concentration with $\nu\kappa/\alpha_s g d^3$ and the other symbols have their usual meanings.

2.2 *The boundary conditions*

The boundary conditions are chosen to simplify the analysis and to fix our attention on the effect of magnetic field and concentration on convection. We assume that the plane surfaces between which the fluid is confined are stress-free and perfect conductors for both heat and salt and they are maintained at constant temperature and concentration so that temperature and concentration perturbations vanish at the boundaries. Also, whenever a magnetic field is present one would match $\mathbf{H}$ to an external vacuum (potential) field tending to H_0 as $|z| \to \infty$ (Chandrasekhar 1961). However, this boundary condition is non-local and almost all work has followed Chandrasekhar in using the boundary condition on magnetic field. So the boundary conditions are:

$$W = \nabla^2 W = 0 \quad \text{at } z = 0, 1, \tag{5}$$

$$T = S = 0 \qquad \text{at } z = 0, 1, \tag{6}$$

$$\mathbf{H} \times \hat{k} = 0 \qquad \text{at } z = 0, 1, \tag{7}$$

where $\hat{k}$ is the unit vector in the z-direction. This choice of boundary conditions has the appealing consequence that the eigenfunctions of the linear stability problem remain proportional to $\exp(in\pi z)$ with n an integer (Rayleigh 1916). Even in the nonlinear regime the idealized free boundary conditions lead to solutions that are periodic in z and seem appropriate in modelling stellar convection.

2.3 *Two-dimensional configuration*

Equations (1)–(4) can be greatly simplified for highly symmetrical configurations. In two-dimensional convection $\mathbf{h}\cdot\hat{\mathbf{j}} = \mathbf{q}\cdot\hat{\mathbf{j}} = 0$ and all physical quantities are assumed to be independent of y in a Cartesian coordinate system (x, y, z). Then the solenoidal fields $\mathbf{q}$ and $\mathbf{h}$ may be expressed in terms of a stream function $\psi(x, z)$ and a flux function (y component of the vector potential) $\phi(x, z)$ such that

$$\mathbf{q} = \left(-\frac{\partial\psi}{\partial z}, 0, \frac{\partial\psi}{\partial x}\right), \quad \mathbf{h} = \left(-\frac{\partial\phi}{\partial z}, 0, \frac{\partial\phi}{\partial x}\right). \tag{8}$$

Substituting (8) in (1)–(4) we may recast the equations in the following form

$$\left(\frac{1}{\sigma}\frac{\partial}{\partial t} - \nabla^2\right)\nabla^2\psi = Q\tau_2\frac{\partial}{\partial z}(\nabla^2\phi) - R_T\frac{\partial T}{\partial x} + R_s\frac{\partial S}{\partial x} + (1/\sigma)J(\psi, \nabla^2\psi) - Q\tau_2 J(\phi, \nabla^2\phi), \tag{9}$$

$$\left(\frac{\partial}{\partial t} - \tau_2\nabla^2\right)\phi = \frac{\partial\psi}{\partial z} + J(\psi, \phi), \tag{10}$$

$$\left(\frac{\partial}{\partial t} - \nabla^2\right)T = -\frac{\partial\psi}{\partial x} + J(\psi, T), \tag{11}$$

$$\left(\frac{\partial}{\partial t} - \tau_1\nabla^2\right)S = -\frac{\partial\psi}{\partial x} + J(\psi, S), \tag{12}$$

where $J(\ldots,\ldots)$ stands for the Jacobian. The idealized boundary conditions on $\mathbf{q}$ and $\mathbf{H}$ may be written in terms of ψ, ϕ, T and S as

$$\psi = \frac{\partial^2\psi}{\partial z^2} = T = S = \frac{\partial\phi}{\partial z} = 0 \text{ at } z = 0, 1, \tag{13}$$

while $\qquad \phi(0, z) = \phi(1/\alpha, z) = 0.$

3. Linear stability analysis

3.1 *The eigenvalue problem*

The criterion for the onset of convection is obtained from the linear stability problem by setting the Jacobian terms in (9)–(12) to zero. To examine the stability of (9)–(12) and

keeping in view of the idealized free boundary conditions we look for the solutions of the form

$$\psi \sim \exp(pt)\sin\pi\alpha x \sin\pi z; \quad T, S \sim \exp(pt)\cos\pi\alpha x \sin\pi z;$$
$$\phi \sim \exp(pt)\sin\pi\alpha x \cos\pi z, \tag{14}$$

where p is the growth rate, $\pi\alpha$ is the horizontal wavenumber and π is the vertical wavenumber. Substituting (14) into (9)–(12) and considering R_T is a free parameter we see that the eigenvalues ($p = i\omega$) satisfy the following equation

$$R_T = \frac{(\tau_1 k^4 + \omega^2)}{(\tau_1^2 k^4 + \omega^2)} R_s + \frac{k^2}{\pi^2\alpha^2}\left[k^4 - \frac{\omega^2}{\sigma} + \pi^2 R_m \frac{(\tau_2 k^4 + \omega^2)}{(\tau_2^2 k^4 + \omega^2)}\right] + i\omega k^2 N, \tag{15}$$

with

$$N = \frac{R_s(\tau_1 - 1)}{\tau_1^2 k^4 + \omega^2} + \frac{k^2}{\pi^2\alpha^2}\left[\frac{\sigma + 1}{\sigma} + \pi^2 R_m \frac{(\tau_2 - 1)}{(\tau_2^2 k^4 + \omega^2)}\right], \tag{16}$$

where $k^2 = \pi^2(\alpha^2 + 1)$. Since R_T is a physical quantity it must be real, so that (16) implies that either $\omega = 0$ or $N = 0$. These conditions help us to study the bifurcation phenomena.

3.2 *Bifurcations from the static solutions*

We first seek the condition for a simple bifurcation: $\omega = 0$. This is traditionally known as an exchange of stabilities. From (15) $\omega = 0$ when $R_T = R_T^{(s)}$, where

$$R_T^{(s)} = \frac{R_s}{\tau_1} + \frac{\pi^4(\alpha^2 + 1)^3}{\alpha^2} + \frac{Q\pi^2(\alpha^2 + 1)}{\alpha^2}. \tag{17}$$

This shows that $R_T^{(s)}$ is minimum for $\alpha = \alpha_c$, where α_c satisfies the equation

$$2\alpha_c^6 + 3\alpha_c^4 = 1 + Q/\pi^2. \tag{18}$$

We see that (18) is the same as the one for single component fluid and is independent of R_s and τ_1 but α_c increases with Q. As $Q \to \infty$, $\alpha_c^2 \to (Q/2\pi^2)^{1/3}$, and

$$R_T^{(e)} = \left(R_T^{(s)} - \frac{R_s}{\tau_1}\right) \sim Q\pi^2.$$

Thus for large Q the Lorentz force favour vertically-elongated cells with motion predominantly along the field lines. Owing to the large value of α_c lateral diffusion becomes extremely effective.

For oscillatory (Hopf-bifurcation, $\omega \neq 0$) neutral solutions (15) requires $N = 0$, which provides a dispersion relation of the form

$$\Delta_1\omega^4 + \Delta_2\omega^2 + \Delta_3 = 0 \tag{19}$$

where

$$\Delta_1 = \frac{k^2(\sigma + 1)}{\sigma} \tag{20}$$

$$\Delta_2 = \pi^2\alpha^2 R_s(\tau_1 - 1) + k^6\frac{(\sigma+1)}{\sigma}(\tau_1^2+\tau_2^2) + \pi^2 k^2 R_m(\tau_2 - 1), \tag{21}$$

$$\Delta_3 = \pi^2\alpha^2 R_s(\tau_1 - 1)\tau_2^2 k^4 + \frac{(\sigma+1)}{\sigma}\tau_1^2\tau_2^2 k^{10} + \pi^2 R_m\tau_1^2(\tau_2 - 1)k^6. \tag{22}$$

One can observe that oscillatory solutions are possible even when these external constraints are acting separately. Though (19) can give rise to more than one positive root, in order to have two positive roots, from Descarte's rule of signs it is necessary that $\Delta_2 < 0$ and $\Delta_3 > 0$, from which it follows that

$$0 < \frac{k^6(\sigma+1)}{\sigma}\tau_2^2 < \pi^2 R_m k^2\frac{(\tau_1+\tau_2)}{\tau_2^2}(\tau_1 - \tau_2)(\tau_2 - 1),$$

which is equivalent to requiring that one of the conditions

$$\tau_1 < \tau_2 < 1 \quad \text{or} \quad \tau_1 > \tau_2 > 1 \tag{23a, b}$$

be satisfied. The important observation from this condition is that oscillatory motions are possible even for τ_1 and τ_2 greater than unity unlike in the single-component systems. The other important observations obtained for different combinations of values of τ_1 and τ_2 are given below.

Case (*i*) $\tau_1 < \tau_2 > 1$

Important information about neutral curves are obtained in the $R_T - \alpha^2$ plane by locating the bifurcation points at which the steady and oscillatory neutral curves join and are shown in figures 1a, b. Also the critical Rayleigh number, R_T^c, following Rudraiah and Shivakumara (1986a), are obtained for $\sigma = 7$, $\tau_1 = 0{\cdot}01$, $\tau_2 = 3$ and are shown in figure 2 and table 2. The lowest locus in figure 2 is the case for $Q = 0$. We see that R_T^c is a piecewise linear function of R_s. At

$$R_s^* = \frac{27\pi^4}{4}\frac{(\sigma+1)\tau_1^2}{\sigma(1-\tau_1)}, \quad \tau_1 < 1,$$

the slope of the $R_T^c - R_s$ plot changes, as does the preferred mode of instability. From this figure it is also clear that the magnetic field inhibits the steady and oscillatory motions to very nearly the same extent (see also table 2). By analogy of the Taylor-Proudman theorem for conducting fluids the effect of magnetic field is to inhibit the onset of stationary convection. But the oscillatory motion is even more strongly inhibited is at first surprising. This is because when $R_s = 0$, oscillatory instability is not possible if $\tau_2 > 1$. Thus it seems logical that in a doubly-diffusive fluid with $\tau_2 > 1$, oscillatory doubly-diffusive instability will be prohibited at Chandrasekhar numbers sufficiently large to dominate the flow.

Case (*ii*) $\tau_1 < \tau_2 < 1$

It is shown that bottom-heavy solute gradient destabilizes the system and this destabilization manifests itself as a minimum in the $R_T - R_s$ plot, as shown in figure 3. From this figure it is clear that the destabilization is associated with an increase in $\omega\tau_2/k^2$, and as $\omega\tau_2/k^2$ goes on increasing, bottom-heavy solute gradient again stabilizes

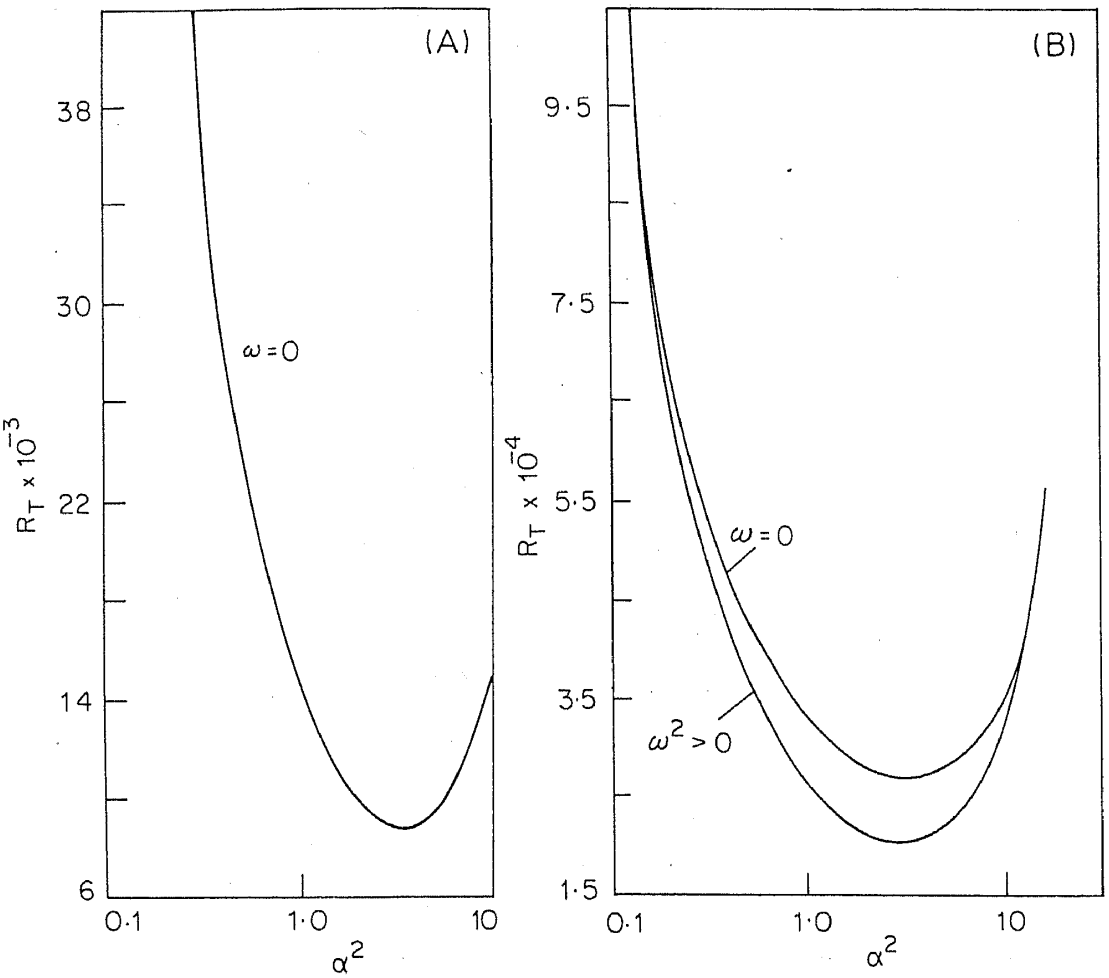

Figure 1. Curves of neutral stability in the R_T-α^2 plane. **(A)** $Q = 1000$, $\tau_1 = 0{\cdot}32$, $R_s = -2000$, $\tau_2 > 1$. **(B)** $Q = 1000$, $\tau_1 = 0{\cdot}32$, $\tau_2 = 1{\cdot}2$, $\sigma = 3{\cdot}0$, $R_s = 4000$.

the fluid layer. This is because the diffusion of solute, for small values of τ_1, is so slow that substantial changes in the bobbing frequency can be produced by changes in R_s that have little stabilizing effect via solute diffusion. Thus, the frequency can be 'tuned' by adjusting R_s. If the frequency is too small, a bobbing parcel will always remain in approximate thermal equilibrium with its environment. If the frequency is too high, no significant heat transfer will occur into or out of the parcel in the first place. In either extreme, the basic overstability mechanism is operating at less than optimal efficiency. At some intermediate frequency, however, the maximum efficiency is achieved, and overstable oscillations set in at a lower value of R_T than is possible for larger or smaller frequencies, i.e. there exists a cut-off frequency below which the system will be stable and above which the system will be unstable. This is consistent with the result shown in figure 3.

Case (iii) $\tau_1 > \tau_2 < 1$

In this part of the parameters range it is observed that the effect of magnetic field is to destabilize the system. This has been shown in figure 4. The existence of such a minimum suggests that this destabilization by magnetic field may have a physical basis

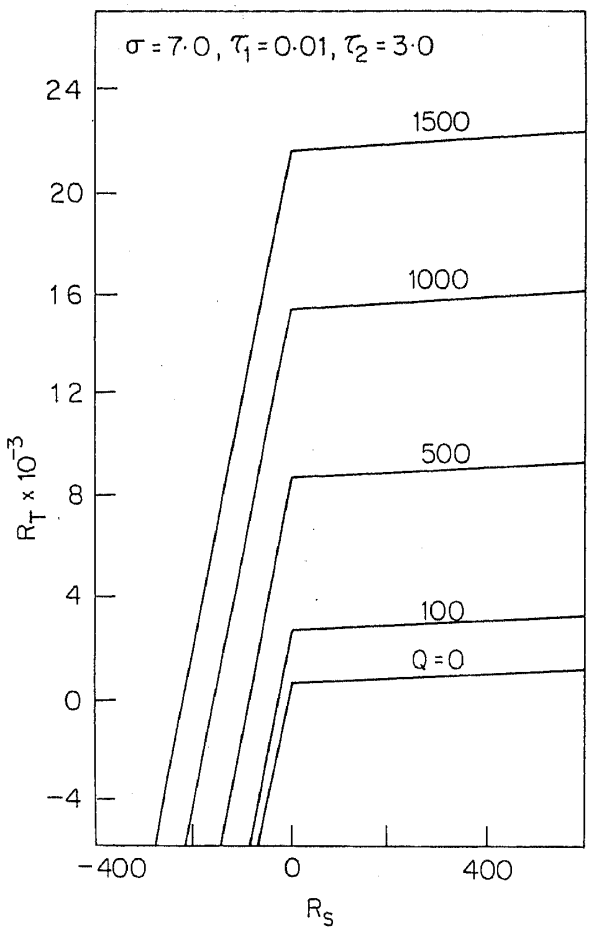

Figure 2. Variation of the critical Rayleigh number R_T with R_s. The portion of each stability boundary lying to the left of the discontinuity in slope corresponds to steady type ($\omega = 0$) while to the right, the onset is oscillatory type ($\omega^2 > 0$).

similar to that of destabilizing effect of a 'stable' density gradient in certain convection problems including the present problem when $\tau_1 < \tau_2 < 1$.

3.3 *Stability boundaries*

In this section we discuss the effect of magnetic field on double-diffusive instabilities diagrammatically in the Rayleigh numbers plane. For this purpose we substitute (14) into (9)–(12) and put $p = i\omega$. Subsequently, by separating the real and imaginary parts and eliminating ω^2 between them we get the following general second degree equation in terms of Rayleigh numbers (see Rudraiah and Shivakumara 1984)

$$a_1 r^2 + a_2 r_s^2 + a_3 r_m^2 + a_4 r r_s + a_5 r r_m + a_6 r_s r_m + a_7 r + a_8 r_s + a_9 r_m + a_0 = 0, \tag{24}$$

where

$$a_i = f_i(\tau_1, \tau_2, \sigma), \quad R_m = Q\tau_2, \ (i = 0 \text{ to } 9)$$

$$(r, r_s) = (R_T, R_s)\pi^2\alpha^2/k^6 \quad \text{and} \quad r_m = R_m\pi^2/k^4,$$

are the normalized Rayleigh and Chandrasekhar numbers. Equation (24) represents

Table 2. Values of the critical thermal Rayleigh number, R_T^c and critical wavenumber, α_c for various values of Q and R_s. The absolute stabilization; $\Delta R_T^c = R_T^c(Q) - R_T^c(0)$ due to magnetic field is also shown. The last column shows the mode of instability. The results are for $\tau_1 = 0{\cdot}01$, $\tau_2 = 3{\cdot}0$ and $\sigma = 7{\cdot}0$.

	Q											
	0		100			500			1000			Mode of instability
R_s	R_T^c	α_c	R_T^c	ΔR_T^c	α_c	R_T^c	ΔR_T^c	α_c	R_T^c	ΔR_T^c	α_c	
−01000	−99342·49	0·7071	−97346·29	1996·20	1·1784	−91421·21	07921·37	1·5909	−84793·00	14549·49	1·8093	Steady
−00100	−09342·49	0·7071	−07346·29	1996·20	1·1784	−01421·12	07921·37	1·5909	05207·00	14549·49	1·8093	Steady
−00010	−00342·49	0·7071	01653·71	1996·20	1·1784	07578·88	07921·37	1·5909	14207·00	14549·49	1·8093	Steady
00000	00657·51	0·7071	02653·71	1996·20	1·1784	08578·88	07921·37	1·5909	15207·00	14549·49	1·8093	Steady
00010	00673·79	0·7071	02686·99	2013·20	1·1785	08656·00	07982·21	1·5884	15331·88	14658·09	1·8044	Oscillatory
00100	00752·66	0·7071	02786·51	2033·85	1·1824	08763·46	08010·80	1·5922	15441·41	14688·75	1·8094	Oscillatory
01000	01541·30	0·7071	03772·76	2231·46	1·2190	09835·45	08294·15	1·6121	16539·68	14998·38	1·8229	Oscillatory
10000	09427·54	0·7071	12946·22	3518·68	1·4689	20219·03	10791·49	1·8234	27344·46	17916·92	1·9685	Oscillatory

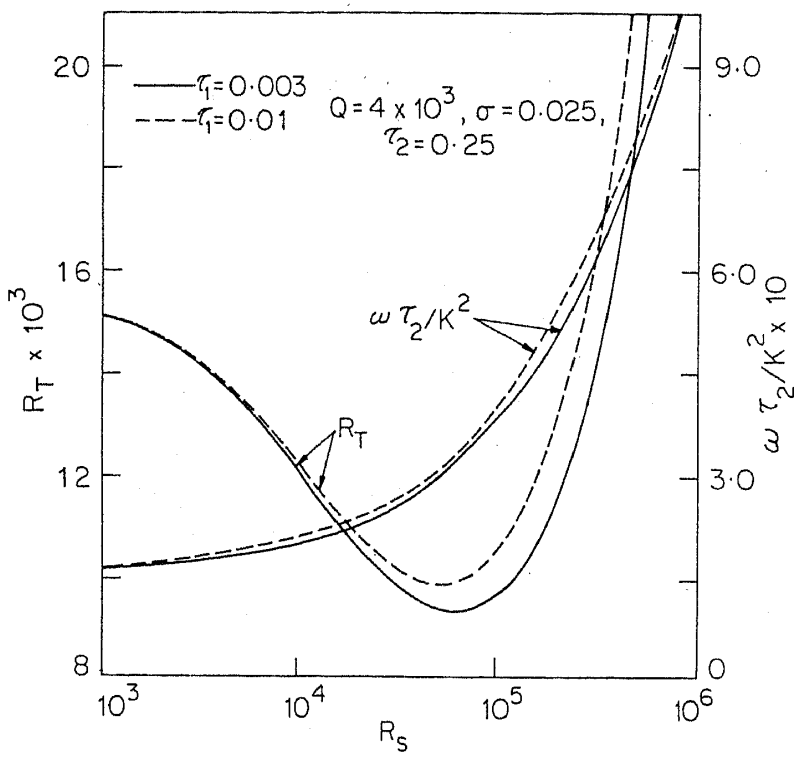

Figure 3. Variation of R_T and $\omega\tau_2/k^2$ with R_s.

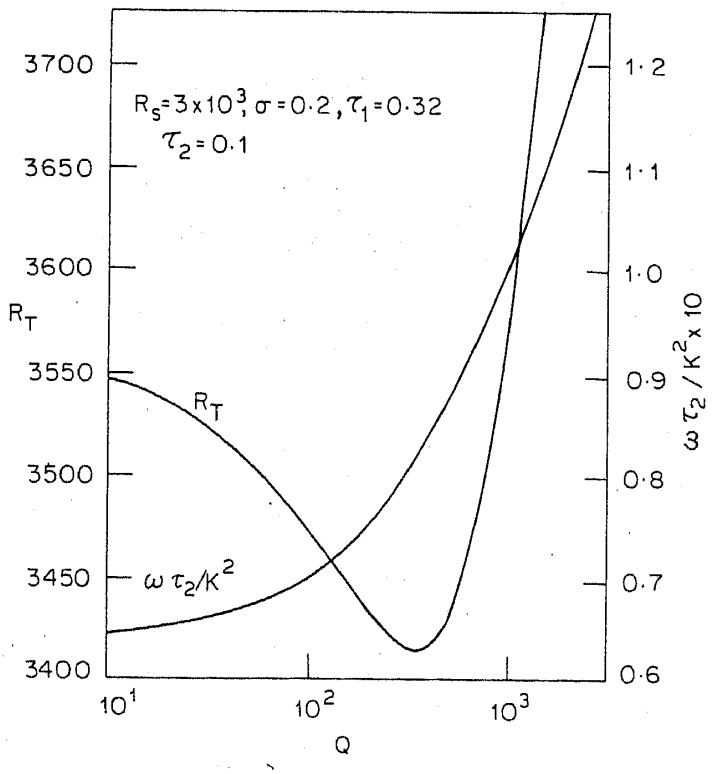

Figure 4. Variation of R_T and $\omega\tau_2/k^2$ with Q.

different surfaces depending on the values of τ_1 and τ_2. For example, for $\tau_1 > 0$ and $\tau_2 < 1$ it represents an hyperboloid denoted by $\mathscr{H}$. The plane surface of marginal stability will be denoted by $\mathscr{P}$. The stability boundaries are drawn considering the following two cases for different values of Q, τ_1 and τ_2 and are shown in figures 5 and 6.

Case (i) τ_1 *and* $\tau_2 \leqslant 1$

In astrophysical and in laboratory models the diffusivity ratios are not far from unity. For example in KCl and NaCl, liquid sodium solutions in the laboratory have diffusivity ratios not far from unity. Here we define the one more plane $\mathscr{S}$ given by

$$r = r_s + r_m.$$

In these figures only the 'relevant portions' of the intersections of $\mathscr{P}$, $\mathscr{H}$ and $\mathscr{S}$ are drawn. The relevant portions mean those which describe a change in the mode of instability for the most unstable mode. Here $\mathscr{H}$ is very closely approximated by its planar asymptotes. The horizontally hatched regions give oscillatory modes and the oblique hatching shows condition unstable to salt-fingers. From figure 5 it is clear that the region of stability increases as Q increases and thus establishing the effect of magnetic field is to inhibit the onset of convection.

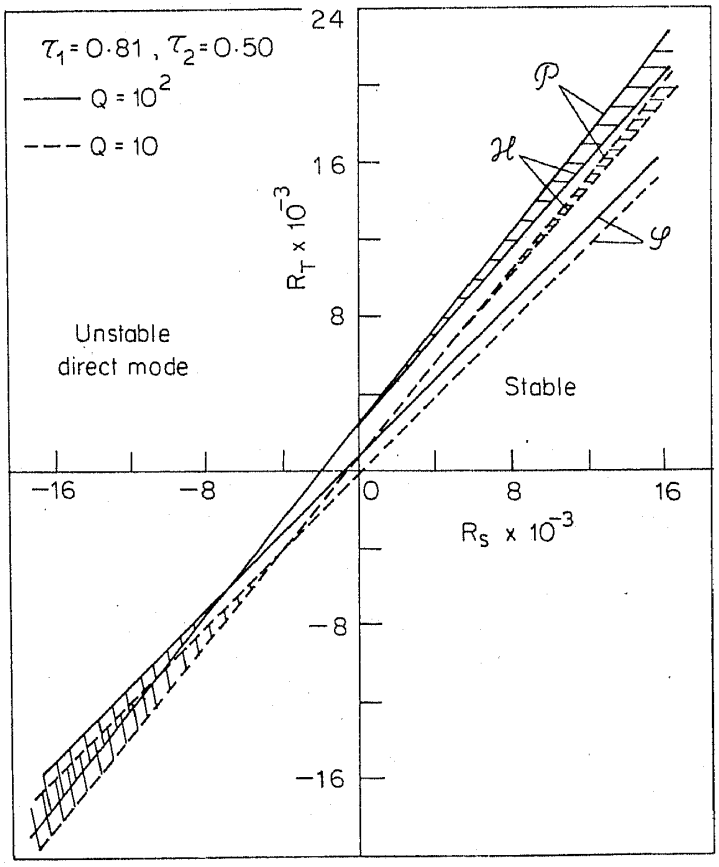

Figure 5. Stability boundaries for different values of Q, τ_2 and τ_1. Horizontally hatched regions give overstable modes. Oblique hatched regions show conditions unstable to salt-fingers.

Case (ii) τ_1 *and* $\tau_2 \ll 1$ $(\tau_1, \tau_2 \to 0)$

In this limit $\mathscr{H}$ approaches its asymptotes and the asymptotes themselves degenerate into a pair of planes given by

$$R_T = \frac{\sigma}{(\sigma+1)}\left(R_s + r_m\pi^4\frac{(\alpha^2+1)^3}{\alpha^2}\right) + \pi^4\frac{(\alpha^2+1)^3}{\alpha^2}, \tag{25}$$

$$R_T = (\tau_1+\tau_2)^{-1}\left(R_s + r_m\pi^4\frac{(\alpha^2+1)^3}{\alpha^2}\right) + \pi^4\frac{(\alpha^2+1)^3}{\alpha^2}, \tag{26}$$

and they satisfy the equations

$$2\alpha^6 + 3\alpha^4 = 1 + \frac{\sigma}{\sigma+1}R_m/\pi^2, \quad 2\alpha^6 + 3\alpha^4 = 1 + (\tau_1+\tau_2)^{-1}\frac{R_m}{\pi^2}. \tag{27}$$

To depict the three-dimensional geometry more clearly the intersections of the surface $\mathscr{P}$ and $\mathscr{S}$ as functions of Q and τ_2 are defined and shown as dotted lines in figure 6. It

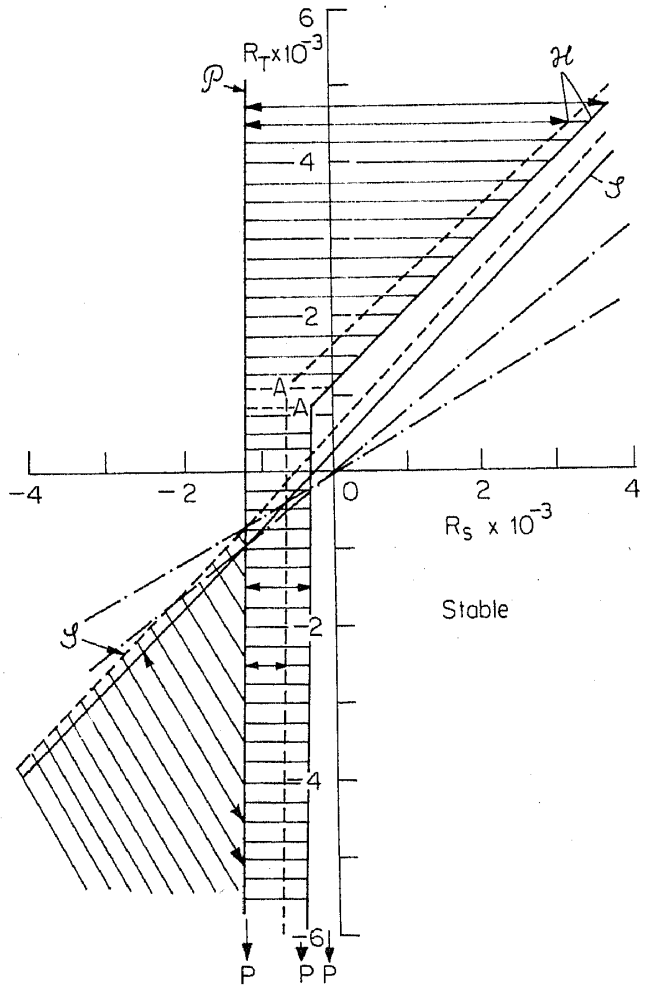

Figure 6. Stability boundaries for the most unstable mode when $\tau_1 = 0{\cdot}01, \sigma = 7, Q = 10^4$, $\tau_2 = 0{\cdot}0025$ and $Q = 10^4, \tau_2 = 0{\cdot}005$ shown (dashed). Hatching and heavy lines have the same meaning as in figure 5; lines are explained in the text.

can be seen that $\mathscr{H}$ is very closely approximated by (25) and (26). The point of intersections of the asymptotes always lies to the right of $\mathscr{P}$. Then the lower asymptote of $\mathscr{H}$ and plane $\mathscr{P}$ converges slowly to intersect at P. The almost vertical lines in the third quadrant are the loci of P as Q and τ_2 are varied. We see that the effect of magnetic field with a minimum τ_2 causes a large extension of the range of values of R_T and R_s at which overstable modes occur.

3.4 *Effect of varying the horizontal wavenumber on stability*

In the previous section we have discussed the stability boundaries considering the situation that α varies with physical parameters. However, to gain more physical insight it is advantageous to vary α by fixing the values of physical parameters and the same is shown in figure 7. In this figure another plane surface $\mathscr{L}$ has been defined, which is the locus of the intersections of $\mathscr{H}$ and $\mathscr{P}$ as α is allowed to vary, to the left of which no wavelengths are overstable and only monotonic instability is possible. To explore the effect of magnetic field further we consider a system which lies in the third quadrant of figure 7 and which always has $\partial\rho/\partial z < 0$. Then, the combined effect of temperature and magnetic field is opposite to that of salinity. When the negative R_s is sufficiently small the system is stable. However, if negative R_s is increased until the $(R_T, -R_s, R_m)$ coordinates cross $\mathscr{H}$ then some wavelengths become overstable beginning at $\alpha^2 = 4{\cdot}218$, the mode which represents a balance between more efficient thermal

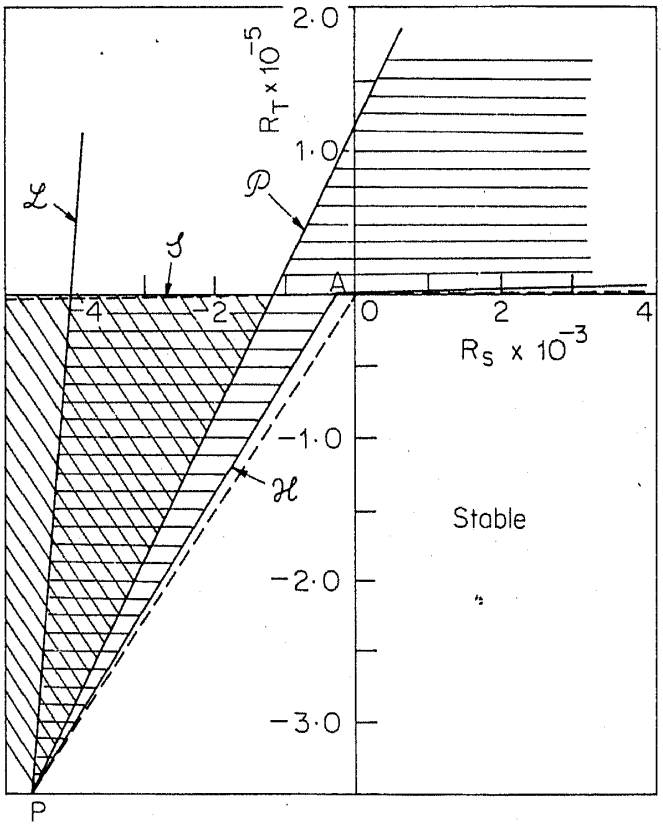

Figure 7. Stability bounds of double-diffusive magnetoconvection for $Q = 10^4$, $\tau_2 = 0{\cdot}0025$, $\sigma = 7$ and $\tau_1 = 0{\cdot}01$. Both oscillatory and salt-finger modes are unstable in the double hatched region.

diffusive, viscous and ohmic damping. Although the oscillatory modes transport components with greater diffusivity more rapidly, here they can transport more concentration by molecular diffusion than the combined heat and magnetic field. If R_s is more destabilizing and the magnetic field is stabilizing but weak so that the conditions are just to the left of $\mathscr{P}$, the mode with wavenumber $\alpha^2 = 4{\cdot}218$ grows monotonically while other modes remain unstable. Now the constraining effects of salinity gradient and magnetic field are large enough to overcome the potential energy released by buoyancy force as well as viscous friction and at larger values all unstable modes to the left of $\mathscr{L}$ are direct. In other words, overstable modes are not possible when a sufficiently large combined salinity gradient and the magnetic field tends to cause the net upward diffusive density flux through oscillatory disturbances.

3.5 *Parametric differentiation method*

In this section we have employed ideas on self-adjoint operators to study the problem of steady, linear double-diffusive magnetoconvection. In particular use of such operators helps in obtaining the behaviour of the critical Rayleigh number with respect to R_s, Q and boundary parameters without doing any numerical evaluation. The key tool that helps in this analysis is the ability to form a self-adjoint operator with respect to certain inner product. We employ a method which has been used by Narayanan (1983, 1984), Shivakumara *et al* (1985), Rudraiah *et al* (1986a) and Rudraiah and Shivakumara (1986a). The first order effects can be calculated using a modified Greens matrix as the kernel of a matrix differential operator (see Friedman 1956).

For this purpose we write (9)–(12) in the following operator form

$$L\mathbf{V} = 0, \tag{28}$$

where

$$L \equiv \begin{bmatrix} \mathscr{D}^2 & R_m \mathscr{D} D & -\pi\alpha R_T^c & \pi\alpha R_s \\ -R_m \mathscr{D} D & -R_m \tau_2 \mathscr{D}^2 & 0 & 0 \\ -\pi\alpha R_0 & 0 & R_T^c & 0 \\ \pi\alpha R_s & 0 & 0 & -R_s \tau_1 \mathscr{D} \end{bmatrix}$$

$$\mathbf{V}^t = [\psi, \phi, T, S] \quad \text{with} \quad D = \partial/\partial z \quad \text{and}$$

$$\mathscr{D}^2 = D^2 - \pi^2\alpha^2.$$

To visualize the variation of R_T^c with R_s, we differentiate (27) with respect to R_s and obtain

$$L\hat{\mathbf{V}} = \hat{\mathbf{h}}, \tag{29}$$

where

$$\hat{\mathbf{h}}^t = [-\pi\alpha S + \hat{R}_T^c \pi\alpha T, 0, 0, 0],$$

and $\hat{}$ represents the derivative with respect to R_s. Defining an inner product in the form

$$\langle \mathbf{a}, \mathbf{b} \rangle = \int_v \mathbf{a}^{*t} \cdot \mathbf{b}\, dv,$$

we can easily show that L and the boundary conditions are self-adjoint. Here v is the domain of the integral operator and asterisk represents complex conjugate. Thus applying a Fredholm alternative condition to (29) we get

$$\hat{R}_T^c \int_v \psi^* T \, dv = \int_v \psi^* S \, dv.$$

This yields the condition that R_T^c increases if R_s increases. Equation (29) can be used to solve for V and we thus obtain the first order effect of an increase in R_s about some known value (say). Similarly we can find out the effect of Q on R_T^c. Finally we consider the effect of boundary parameters on R_T^c because our earlier analysis is for the special case of Biot and Sherwood numbers going to infinity. Proceeding as before one will get after much algebraic manipulation

$$\pi\alpha \frac{\bar{R}_T^c}{R_T^c} \int_p \psi^* T \, dv = \int_v -|T|^2 \, dv. \tag{30}$$

On using the energy equation we get from (30)

$$\frac{\partial}{\partial \mathrm{Bi}} (\ln R_T^c) > 0,$$

where Bi is a Biot number. Thus if $R_T^c < 0$ (such as heated from above) then R_T^c will decrease with an increase in Bi. In most cases we are concerned with the case of heating from below and so the case of $\mathrm{Bi} \to \infty$ provides an upper bound on R_T^c. Similar results are true in the case of Sherwood number.

4. Two-dimensional double-diffusive magnetoconvection in a truncated model

In recent years (see Da Costa *et al* 1981; Knobloch and Weiss 1983 and references therein) considerable interest has been evinced in nonlinear fluid dynamical problems that exhibit a transition from periodic oscillations to behaviour that is apparently chaotic. In particular much attention has been focussed on systems in which a sequence of periodic-doubling bifurcations is followed by aperiodic oscillations. Knobloch and Weiss (1983) examined the behaviour of one such system, considering a model of magnetoconvection in a single-component fluid. Recently, Rudraiah and Shivakumara (1986a) explored the behaviour of one such system, derived as a model of double-diffusive magnetoconvection in the presence of an imposed vertical magnetic field. With the available computer facilities in Bangalore, it was not possible for them to solve the full nonlinear partial differential equations (1) to (4) with sufficient accuracy to determine whether such a sequence of bifurcations actually occurs for thermohaline magnetoconvection. Therefore, instead of dealing with the full problem, Rudraiah and Shivakumara (1986a) studied the two-dimensional problem using a truncated model approach put forward by Veronis (1966). They solved this model problem, consisting of seven coupled nonlinear ordinary differential equations, by a combination of analytical and numerical techniques. In this section we briefly review this problem.

4.1 *Finite amplitude analysis with limited representation*

A minimal system which describes finite amplitude convection is taken as

$$\psi = A(t)\sin\pi\alpha x \sin\pi z, \tag{31}$$

$$T = B(t)\cos\pi\alpha x \sin\pi z + C(t)\sin 2\pi z, \tag{32}$$

$$S = D(t)\cos\pi\alpha x \sin\pi z + E(t)\sin 2\pi z, \tag{33}$$

$$\phi = F(t)\sin\pi\alpha x \cos\pi z + G(t)\sin 2\pi\alpha x, \tag{34}$$

where the amplitudes A to G are functions of time and are to be determined by the dynamics of the system. Substituting (31)–(34) into (9)–(12) and equating the coefficients of like terms we get the following generalized Lorenz model:

$$\frac{k^2}{\sigma}\frac{dA}{dt} = -k^4 A - \pi^3 R_m(\alpha^2+1)F - \pi\alpha R_T B + \pi\alpha R_s D + \pi^4 R_m \alpha(3\alpha^2-1)FG, \tag{35}$$

$$dB/dt = -k^2 B - \pi\alpha A - \pi^2\alpha AC, \tag{36}$$

$$dC/dt = -4\pi^2 C + \frac{\pi^2\alpha AB}{2}, \tag{37}$$

$$dD/dt = -\tau_1 k^2 D - \pi\alpha A - \pi^2\alpha AE, \tag{38}$$

$$dE/dt = -4\pi^2\tau_1 E + \frac{\pi^2\alpha AD}{2}, \tag{39}$$

$$dF/dt = -\tau_2 k^2 F + \pi A + \pi^2\alpha AG, \tag{40}$$

$$dG/dt = -4\pi^2\alpha^2\tau_2 G - \frac{\pi^2\alpha AF}{2}. \tag{41}$$

This seventh order model of double-diffusive magnetoconvection provides, as in the case of single component magnetoconvection (Knobloch and Weiss 1983) and double-diffusive convection (Huppert and Moore 1976, Da Costa *et al* 1981), a good example whose solutions are qualitatively similar to those of the partial differential equations from which they are derived.

4.2 *Steady finite amplitude convection*

For steady case ($\partial/\partial t = 0$), the above set of equations reduce to algebraic equations. After eliminating all amplitudes, except A, yields

$$A\left[\left(\frac{A^2}{8}\right)^4 + \left(\frac{k^2}{\pi^2\alpha^2}\right)c_0\left(\frac{A^2}{8}\right)^3 + \left(\frac{k^2}{\pi^2\alpha^2}\right)^2 c_1\left(\frac{A^2}{8}\right)^2 + \left(\frac{k^2}{\pi^2\alpha^2}\right)^3 c_2\left(\frac{A^2}{8}\right) + \tau_1^2\tau_2^2\alpha^4\left(\frac{k^2}{\pi^2\alpha^2}\right)^4 c_3\right] = 0, \tag{42}$$

where

$$c_i = f_i(\alpha, Q, R_T, R_s, \tau_1, \tau_2, \sigma), \quad (i = 0 \text{ to } 3).$$

By solving (42) we can find the amplitude. Once we know the amplitude the heat and mass transport can be calculated by the relations

$$\mathrm{Nu} = Hd/\kappa\Delta T = 1 - 2\pi C, \tag{43}$$

and

$$\mathrm{Nu}_s = 1 - 2\pi E. \tag{44}$$

The results obtained for certain physical parameters are shown in figure 8. It is clear that the effect of magnetic field is to reduce the heat and mass transport.

4.3 *Oscillatory finite amplitude convection by numerical experiments*

In this section, the behaviour of nonlinear periodic solutions is investigated more generally by integrating (35)–(41) numerically using Runge-Kutta-Gill method satisfying the following initial conditions:

$$A = 0{\cdot}1,\ B = 1,\ C = 0,\ D = 1,\ E = 0,\ F = 1 \text{ and } G = 0. \tag{45}$$

We observe that the system possesses an important symmetry, for it is invariant under the transformation

$$(A, B, C, D, E, F, G) \rightarrow (-A, -B, C, -D, E, -F, G).$$

Also, the equations describe a contraction mapping in the seven-dimension space because

$$\frac{\partial \dot{A}}{\partial A} + \frac{\partial \dot{B}}{\partial B} + \frac{\partial \dot{C}}{\partial C} + \frac{\partial \dot{D}}{\partial D} + \frac{\partial \dot{E}}{\partial E} + \frac{\partial \dot{F}}{\partial F} + \frac{\partial \dot{G}}{\partial G} < 0,$$

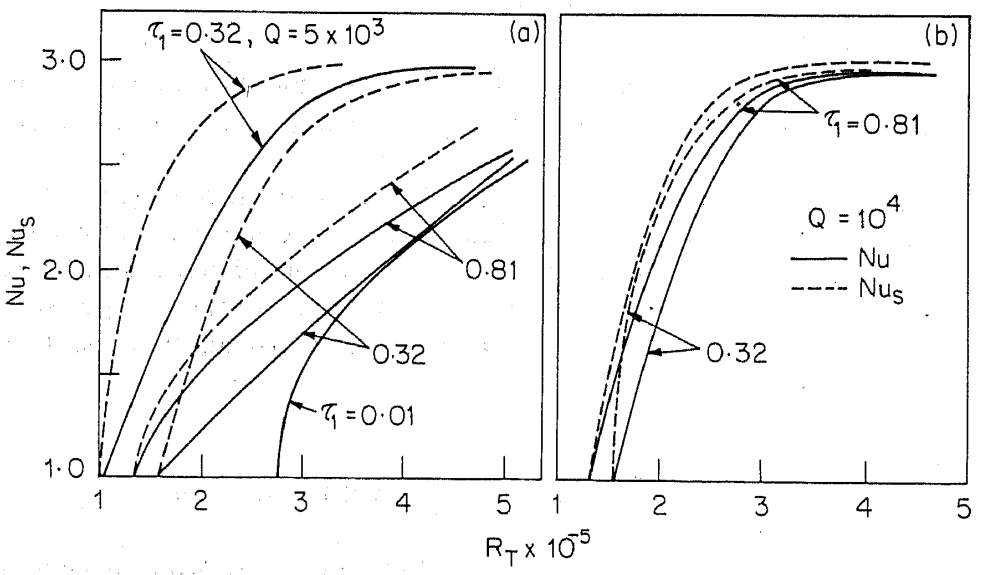

Figure 8. Nu and Nu_s vs R_T for $R_s = 10^4$ at two values of τ_2. **(a)** $\tau_2 = 0{\cdot}5$ and **(b)** $\tau_2 = 0{\cdot}25$.

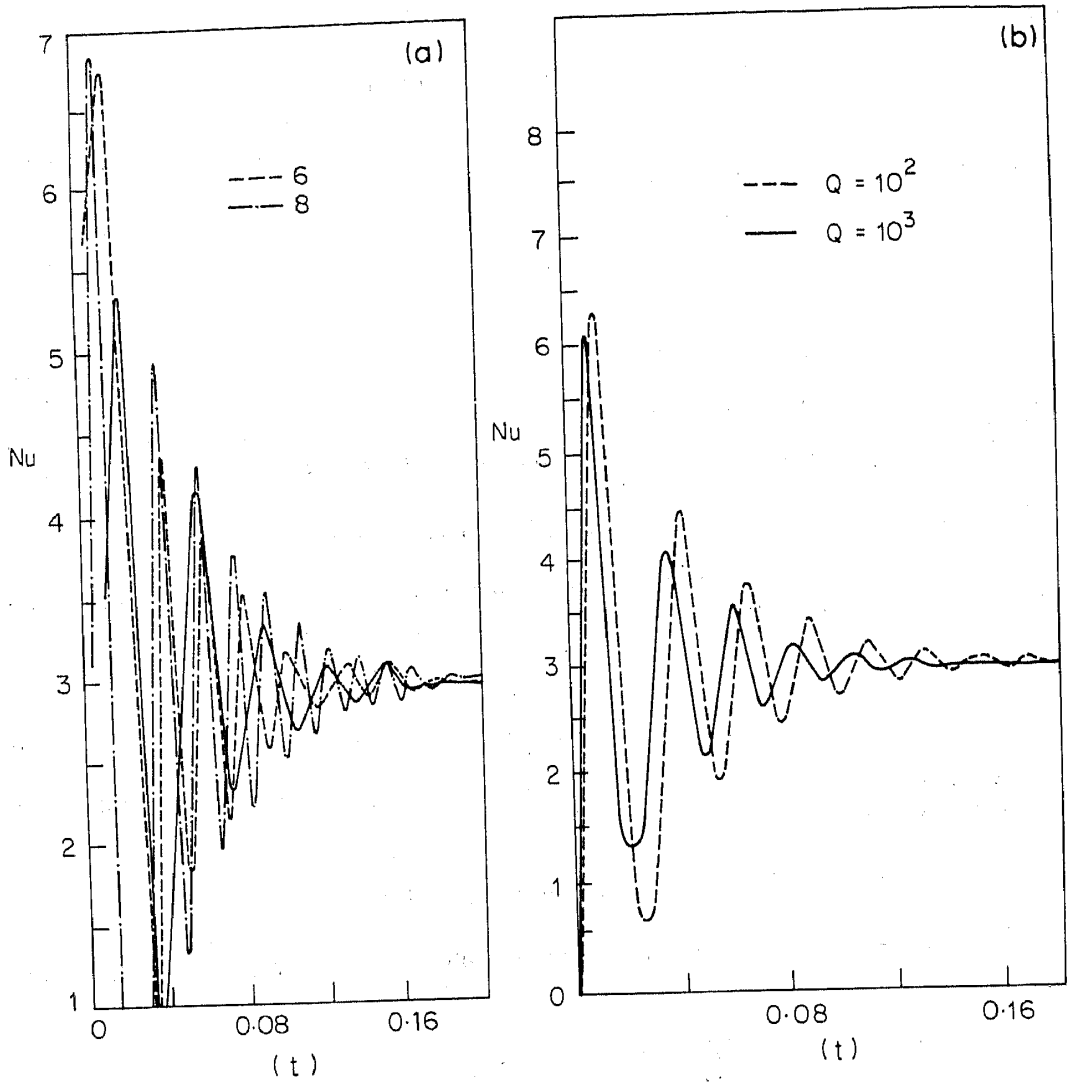

Figure 9. Variation of Nusselt number with time (t) for **a.** $Q = 10^2$, $R_s = 10^4$, ——$R_T/R_T^s = 2$, $\tau_1 = 0{\cdot}32$, $\tau_2 = 0{\cdot}5$ and $\sigma = 0{\cdot}2$. **b.** $R_s = 10^4$, $\tau_1 = 0{\cdot}32$, $\tau_2 = 0{\cdot}5$, $\sigma = 0{\cdot}2$ and $R_T = 4R_T^C$.

where the dots denote derivatives w.r.t. time t. From the above argument it implies that the trajectories may be attracted to fixed points, to limit cycles or possibly, to a strange attractor.

The results obtained from this numerical study are depicted in figures 9a and 9b. It is found that the steady state reaches via a transient state and an increase in the Rayleigh number is to make the system more unsteady. Also our numerical study compares well with the corresponding steady state analytical results of the previous section. From figure 9b, it is clear that the effect of magnetic field is to dampen the oscillations and to reduce the heat transport.

5. Finite amplitude steady convection by perturbation theory

The analysis studied in the previous section is only two-dimensional and no attempt was made to determine the quantitative results for general representation with different

cell pattern. Therefore, in this section we determine the finite amplitude solutions and in turn the preferred cell pattern considering both two- and three-dimensional motions using the perturbation technique of Malkus (see Malkus and Veronis 1958; Rudraiah 1981; Rudraiah and Shivakumara 1986b).

5.1 *Perturbation equations*

It is known that in the neighbourhood of the simple bifurcation at $R_T^{(s)}$ there exists non-trivial steady solutions corresponding to finite-amplitude convection. The linear theory presented earlier does not, however, tell us whether these solutions will be stable. We therefore introduce a small parameter ε such that any dependent variable can be expressed as perturbation series of the form say

$$f = \varepsilon f_0 + \varepsilon^2 f_1 + \varepsilon^3 f_2 + \ldots,$$

and

$$R_T = R_T^{(c)} + \varepsilon R_{T_1} + \varepsilon^2 R_{T_2} + \ldots, \tag{46}$$

where R_{T_i} are integral functions of W_i, T_i, S_i and h_i (Malkus and Veronis 1958; Veronis 1959). At each stage in the expansion we may define a column vector

$$\mathbf{A}_n = [W_n, T_n, S_n, h_{z_n}, \eta_n, \xi_n]^t, \tag{47}$$

where $\eta = (\partial v/\partial x) - (\partial u/\partial y)$ and $\xi = (\partial h_y/\partial x) - (\partial h_x/\partial y)$ are the z-component of vorticity and current density. If we substitute (46) into (1)–(4) then at leading order in ε the equations are linear and can be written in the compact form

$$\mathscr{L}\mathbf{A}_0 = 0, \tag{48}$$

where

$$\mathscr{L} \equiv \begin{bmatrix} L_1 & 0 & 0 & 0 & 0 & 0 \\ -R_T^{(c)} & -\nabla^2 & 0 & 0 & 0 & 0 \\ -R_s/\tau_1 & 0 & -\nabla^2 & 0 & 0 & 0 \\ -\dfrac{1}{\tau_2}\dfrac{\partial}{\partial z} & 0 & 0 & -\nabla^2 & 0 & 0 \\ 0 & 0 & 0 & 0 & L_2 & 0 \\ 0 & 0 & 0 & 0 & \tau_2^{-1}\dfrac{\partial}{\partial z} & -\nabla^2 \end{bmatrix},$$

with

$$L_1 = \tau_1\tau_2\nabla^4\left\{\nabla^6 - (R_T^{(c)} - R_s/\tau_1)\nabla_1^2 - \frac{R_m}{\tau_2}\nabla^2 - \partial^2/\partial z^2\right\},$$

$$L_2 = \nabla^2 - \frac{R_m}{\tau_2}\frac{\partial^2}{\partial z^2}.$$

To second order in ε we obtain

$$\mathscr{L}\mathbf{A}_1 \equiv \begin{bmatrix} \tau_1\tau_2\nabla^4(R_{T_1}\nabla_1^2 W_0 - \nabla^2\left(\frac{III_{00}}{\sigma} - R_m V_{00}\right) - \nabla_1^2(I_{00} - II_{00}) - \frac{R_m}{\tau_2}\nabla^2\frac{\partial}{\partial z}VI_{00} \\ R_{T_1}W_0 - I_{00} \\ -II_{00}/\tau_1 \\ -\frac{1}{\tau_2}\{VI_{00}\} \\ \frac{R_m}{\tau_2}\frac{\partial}{\partial z}\{VIII_{00} - IX_{00}\} + \frac{1}{\sigma}\nabla^2 IV_{00} - R_m\nabla^2 VII_{00} \\ \frac{1}{\tau_2}\{VIII_{00} - IX_{00}\}. \end{bmatrix}$$

Similarly, the higher order equations may be obtained where *I–IX* represent nonlinear terms and $\mathbf{A}_n (n = 0, 1, 2)$ differs for different planforms.

6. Analysis for two-dimensional motion with free surfaces

In this case we assume that all the dependent variables are independent of the y-coordinate. Though the two-dimensional motion is an approximation, it represents a simple type of motion with minimum mathematics.

6.1 *Finite amplitude solution for rolls*

The solution to the stability problem (48) is given by

$$\begin{aligned} \mathbf{A}_0 = 2 \quad & [\cos\pi\alpha x \sin\pi z,\ R_0 \cos\pi\alpha x \sin\pi z,\ \tau_1 R_0 \cos\pi\alpha x \sin\pi z, \\ & (1/\tau_2\pi(\alpha^2+1))\cos\pi\alpha x \cos\pi z,\ -(1/\alpha)\sin\pi\alpha x \cos\pi z,\ 0, \\ & (1/\tau_2\pi\alpha(\alpha^2+1)\sin\pi\alpha x \sin\pi z, 0]^t. \end{aligned} \tag{49}$$

where $(R_0, R_0^*) = (R_T^{(c)}, R_s/\tau_1^2)/\pi^2(\alpha^2+1)$ and the values of $R_T^{(c)}$ and α_c corresponding to a given value of Q are given by (17) and (18) respectively. The equations for higher order approximations are non-homogeneous and the solutions of these equations pose a problem because of the presence of resonance and secular terms. So R'_{T_i} are evaluated in such a way that they eliminate the resonant inhomogeneous terms. Also the expansion procedure that we have used here show that $w_i (i > 0)$ must be orthogonal to w_0 but need not be mutually orthogonal. This procedure leads to

$$\mathbf{A}_1 = \left[0, 0, 0, \frac{\cos 2\pi\alpha x}{\tau_2^2\pi^2\alpha^2(\alpha^2+1)}, 0, 0, 0, 0\right]^t \quad \text{and} \quad R_{T_1} = 0.$$

Proceeding like this we get the first finite amplitude result as

$$R_{T_2} = \frac{1}{2\alpha^2}\left[\pi^2(\alpha^2+1)^2 + \left(\frac{R_m}{\tau_2} + \frac{2(\alpha^2-1)R_m}{\tau_2^3\alpha^2(\alpha^2+1)}\right)\right] + \frac{R_s(\tau_1^2-1)}{2\tau_1^3\pi^2(\alpha^2+1)}. \tag{50}$$

This equation for a single component fluid ($R_s = 0$) agrees with Weiss (1981a) except for

Table 3. Values of Q_c^m with $R_T = 10^4$.

τ_1	R_s ($\times 10^3$)	Q_c^m
—	0	604·26
0·32	1	378·03
0·32	2	167·29
0·81	1	513·57
0·81	2	424·53

a change in the multiplication factor due to the different normalization employed in the two cases. This expression also shows that R_{T_2} may be either positive or negative depending on the values of τ_2, α^2, R_s, Q and τ_1 and hence subcritical motions are possible for certain values of parameters and for other values supercritical motions are possible.

It is of interest to study the effect of increase in Q while R_T and R_s are held fixed. We see that for fixed values of R_T and R_s convection sets in when

$$Q^m = \frac{(R_T - R_s/\tau_1)\alpha^2}{\pi^2(\alpha^2+1)} - \pi^2(\alpha^2+1)^2, \tag{51}$$

provided $\alpha = \alpha_c$ satisfies the equation

$$\alpha_c^2 = \left\{\frac{(R_T - R_s/\tau_1)}{2\pi^4}\right\}^{1/3} - 1. \tag{52}$$

Table 3 gives the value of Q_c^m for two values of R_s and τ_1.

For a single-component system the value of Q_c^m, coincides with the value of Weiss (1981b).

7. Analysis for three-dimensional motion with free surfaces

The iterative method used in the previous section to study the local nonlinear stability of this problem is now extended to three-dimensional motion, with the object of determining the preferred cell pattern. This is investigated in this section by considering general rectangle (i.e. square cells and limiting rectangles) and hexagonal planforms.

7.1 *Finite amplitude solution for general rectangular cells*

The solution to the stability problem (48) is given by

$$\begin{aligned}\mathbf{A}_0 = 2\sqrt{2}\,[&\cos\pi lx\cos\pi my\sin\pi z,\ R_0\cos\pi lx\cos\pi my\sin\pi z,\\ &\tau_1 R_0^*\cos\pi lx\cos\pi my\sin\pi z,\ \{1/\tau_2\pi(\alpha^2+1)\}\times\\ &\cos\pi lx\cos\pi my\cos\pi z,\ -(l/\alpha^2)\sin\pi lx\cos\pi my\cos\pi z,\\ &-(m/\alpha^2)\cos\pi lx\sin\pi my\cos\pi z,\ l/\{\tau_2\pi\alpha^2(\alpha^2\\ &+1)\sin\pi lx\cos\pi my\sin\pi z,\ m/\{\tau_2\pi\alpha^2(\alpha^2\\ &+1)\}\cos\pi lx\cos\pi my\cos\pi z]^t,\end{aligned} \tag{53}$$

where $l^2+m^2+\alpha^2$ and $2\sqrt{2}$ is the normalization constant. Proceeding as before we obtain $R_{T_1}=0$ and R_{T_2} can be obtained in the form

$$R_{T_2}=\tfrac{1}{2}(R_0-R_0^*/\tau_1)-\frac{\pi}{2\alpha^2}\{m^2(b_1-c_1)+l^2(b_2-c_2)\}$$
$$+\frac{\pi^3}{2\alpha^4}(m^2a_1+l^2a_2)\left\{\frac{R_m/\tau_2^2}{\pi^2}-\frac{(\alpha^2+1)^2}{\sigma}\right\}$$
$$+\frac{\pi R_m(\alpha^2+1)}{2\tau_2^2\alpha^4}\left\{\frac{m^2a_1}{l^2+1}+\frac{l^2a_2}{m^2+1}+\frac{5\alpha^2-1}{\pi\tau_2(\alpha^2+1)^2}\right\}, \tag{54}$$

where

$$a_1(l,m)=-\frac{8\pi^3l^2m^2\alpha^{-2}\left[R_0-R_0^*+4\alpha^{-2}(l^2+1)\left\{\frac{\pi^2(\alpha^2+1)}{\sigma}+\frac{R_m(\alpha^2+1)^{-1}}{\tau_2^2}\right\}\right]}{64\pi^6(l^2+1)^3+16R_m\pi^4(l^2+1)/\tau_2-4\pi^2l^2(R_T^{(c)}-R_s/\tau_1)},$$

$$b_1(l,m)=\frac{R_T^{(c)}a_1(l,m)-2R_0m^2\alpha^{-2}\pi}{4\pi^2(l^2+1)},$$

$$c_1(l,m)=\frac{R_sa_1(l,m)/\tau_1-2R_0^*\pi m^2\alpha^{-2}}{4\pi^2(l^2+1)}$$

$a_2(l,m)=a_1(m,l)$, $b_2(l,m)=b_1(m,l)$ and $c_2(l,m)=c_2(m,l)$. Since (54) is a function of Q,τ_2,R_s,τ_1 and l/m, we have infinite set of values. Here we restrict our attention to the values of parameters which are the same as that of rolls. However, l/m cannot be chosen arbitrarily. Rudraiah (1981) has shown how to select its proper value using the relative stability criterion. We choose such values in computing R_2 and the heat and mass transport.

7.2 *Finite amplitude solution for hexagonal cells*

In this section we study convection by hexagonal cell pattern which has one additional degree of freedom compared to the general rectangular cell patterns discussed in the previous section. The complete solution to the first order problem is given by

$$\mathbf{A}_0=\frac{2}{\sqrt{3}}\left[\phi_1\sin\pi z,\ R_0\phi_1\sin\pi z,\ R_0^*\phi_1\sin\pi z,\ 1/\{\tau_2\pi(\alpha^2+1)\}\,\phi_1\cos\pi z\right.$$
$$-(\sqrt{3}/\alpha)\sin\left(\frac{2\pi}{\sqrt{3}L}x\right)\cos\left(\frac{2\pi}{3L}y\right)\cos\pi z-(1/\alpha)\phi_2\cos\pi z,$$
$$\sqrt{3}/\{\tau_2\pi\alpha(\alpha^2+1)\}\sin\left(\frac{2\pi}{\sqrt{3}L}x\right)\cos\left(\frac{2\pi}{3L}y\right)\sin\pi z,$$
$$\left.1/\{\tau_2\pi\alpha(\alpha^2+1)\}\right]^t,$$

where

$$\phi_1=2\cos\left(\frac{2\pi}{\sqrt{3}L}x\right)\cos\left(\frac{2\pi}{3L}y\right)+\cos\left(\frac{4\pi}{3L}y\right),$$

$$\phi_2 = \cos\left(\frac{2\pi}{\sqrt{3}L}x\right)\sin\left(\frac{2\pi}{3L}y\right)+\sin\left(\frac{4\pi}{3L}y\right),$$

and $L = 4/3\alpha$ is the non-dimensional length of one side of the hexagon. As before we found that $R_{T_1} = 0$ and R_{T_2} is evaluated and is given by

$$R_{T_2} = \tfrac{1}{2}(R_0 - R_0^*/\tau_1)+\frac{3\pi}{4}(D_3 - D_1)+\frac{\pi}{4}(D_4 - D_2)$$

$$-\frac{3D_5}{4\pi^2\alpha^2\sigma}-\frac{3\pi R_m}{4\tau_2^2\alpha^2 R_0}(D_1 + D_2), \tag{55}$$

where

$$D_i = f_i(\alpha, \tau_2, \tau_1, Q, R_s) \quad (i = 1 \text{ to } 5).$$

The convective heat and mass transport is calculated and discussed in the next section.

8. Convective heat and mass transport

To know explicitly the effects of magnetic field and salinity gradient on heat and mass transfer, it is of interest to study the heat and mass transfer measured by the Nusselt numbers for heat (Nu) and solute (Nu_s) defined by

$$\begin{aligned} \mathrm{Nu} &= 1 + (1/R_T)\{W_T\}_m, \\ \mathrm{Nu}_s &= 1 + (1/R_s)\{W_s\}_m. \end{aligned} \tag{56}$$

In this equation, the second term represents convective heat and mass transport. To the ε^2-approximation

$$\begin{aligned} \mathrm{Nu} &= 1+\frac{R_0}{R_{T_2}}(1 - R_T^{(c)}/R_T), \\ \mathrm{Nu}_s &= 1+\frac{R_0}{R_{T_2}\tau_1^2}\left(\frac{R_T}{R_T^{(c)}}-1\right). \end{aligned} \tag{57}$$

We see that the convective heat and mass transfer vary inversely as R_{T_2} and the values calculated for different planforms are tabulated in tables 4, 5 and 6 for some values and for other values curves are drawn. From these tables we arrived at the following general conclusions:

(i) The value of the heat transport for limiting rectangles differs markedly from that of rolls. This discrepancy may be due to the fact that the rectangles are normalized differently from the rolls.

(ii) A definite qualitative result can be made out from the heat transport of mercury where we see that finite amplitude instability cannot occur throughout the range of Q considered for $R_s = 10^3$ and $\tau_1 = 0{\cdot}81$.

(iii) Another interesting result is that the convective heat transport for both the square cells ($l/m = 1$) and limiting rectangles ($l/m = \infty$) approach asymptotic values for large Q and $\tau_2 \geqslant 0{\cdot}8$. The asymptotic value for square cells is equal to the value for rolls.

Table 4. Convective heat and mass (the upper value in each pair) transport for $R_s = 1000$ and $\tau_1 = 0{\cdot}32$.

	$\tau_2 = 0{\cdot}25$				$\tau_2 = 0{\cdot}50$			
Q	Rolls	Squares	Lim. Rect.	Hexagons	Rolls	Squares	Lim. Rect.	Hexagons
1·0E−04	−7·3055E−01	−6·1357E−01	−4·8703E−01	−6·8174E−01	−7·3055E−01	−6·1356E−01	−4·8703E−01	−6·8174E−01
	−2·8296E−01	−2·3765E−01	−1·8864E−01	−2·6406E−01	−2·8296E−01	−2·3765E−01	−1·8864E−01	−2·6406E−01
1·0E−02	−7·3038E−01	−6·1377E−01	−4·8715E−01	−6·8176E−01	−7·3051E−01	−6·1363E−01	−4·8707E−01	−6·8176E−01
	−2·8292E−01	−2·3775E−01	−1·8870E−01	−2·6409E−01	−2·8297E−01	−2·3769E−01	−1·8867E−01	−2·6408E−01
1·0E+00	−7·1647E−01	−6·3419E−01	−4·9919E−01	−6·8330E−01	−7·2757E−01	−6·1989E−01	−4·9042E−01	−6·8312E−01
	−2·7965E−01	−2·4754E−01	−1·9484E−01	−2·6670E−01	−2·8398E−01	−2·4195E−01	−1·9142E−01	−2·6664E−01
1·0E+01	−6·8147E−01	−8·4421E−01	−6·1994E−01	−6·9692E−01	−7·2292E−01	−6·7040E−01	−5·1870E−01	−6·9392E−01
	−2·8248E−01	−3·4994E−01	−2·5698E−01	−2·8889E−01	−2·9967E−01	−2·7790E−01	−2·1501E−01	−2·8765E−01
1·0E+02	−1·0628E+00	1·4781E+00	1·6874E+00	−8·8315E−01	−8·4374E−01	−1·0907E+00	−7·8320E−01	−7·9860E−01
	−6·2891E−01	8·7464E−01	9·9853E−01	−5·2260E−01	−4·9928E−01	−6·4540E−01	−4·6345E−01	−4·7256E−01
1·0E+03	3·5629E−01	1·3187E−01	9·3823E−02	8·0667E−01	4·2779E+00	7·4599E−01	5·0950E−01	5·9976E+00
	6·6882E−01	2·4754E−01	1·7612E−01	1·5143E+00	8·0305E+00	1·4004E+00	9·5643E−01	1·1259E+01
1·0E+04	4·2718E−02	2·6077E−02	1·6798E−02	6·1608E−02	1·0636E−01	7·6727E−02	4·9486E−02	1·0263E−01
	5·3786E−01	3·2833E−01	2·1149E−01	7·7570E−01	1·3392E+00	9·6606E−01	6·2307E−01	1·2922E+00
1·0E+05	6·9015E−03	5·0261E−03	3·1246E−03	8·7125E−03	1·3058E−02	1·1149E−02	7·1150E−03	1·2457E−02
	7·6434E−01	5·5664E−01	3·4605E−01	9·6490E−01	1·4461E+00	1·2348E+00	7·8798E−01	1·3796E+00
1·0E+06	1·0463E−03	8·5142E−04	5·2947E−04	1·2067E−03	1·5806E−03	1·4592E−03	9·4094E−04	1·5235E−03
	1·1018E+00	8·9660E−01	5·5757E−01	1·2708E+00	1·6645E+00	1·5367E+00	9·9088E−01	1·6043E+00
1·0E+07	1·3975E−04	1·2348E−04	7·8175E−05	1·5142E−04	1·7699E−04	1·7019E−04	1·1124E−04	1·7309E−04
	1·4394E+00	1·2718E+00	8·0515E−01	1·5595E+00	1·8229E+00	1·7529E+00	1·1457E+00	1·7827E+00
1·0E+08	1·6574E−05	1·5487E−05	1·0003E−05	1·7283E−05	1·8756E−05	1·8408E−05	1·2145E−05	1·8536E−05
	1·6898E+00	1·5790E+00	1·0198E+00	1·7620E+00	1·9123E+00	1·8767E+00	1·2382E+00	1·8898E+00
1·0E+09	1·8150E−06	1·7534E−06	1·1491E−06	1·8530E−06	1·9295E−06	1·9125E−06	1·2685E−06	1·9182E−06
	1·8418E+00	1·7793E+00	1·1660E+00	1·8804E+00	1·9580E+00	1·9407E+00	1·2872E+00	1·9465E+00

Table 5. Convective heat and mass (the upper value in each pair) transport for $R_s = 1000$ and $\tau_1 = 0{\cdot}32$.

	$\tau_2 = 0{\cdot}80$				$\tau_2 = 5{\cdot}00$			
Q	Rolls	Squares	Lim. Rect.	Hexagons	Rolls	Squares	Lim. Rect.	Hexagons
1·0E−04	−7·3055E−01	−6·1356E−01	−4·8703E−01	−6·8174E−01	−7·3055E−01	−6·1356E−01	−4·8703E−01	−6·8174E−01
	−2·8296E−01	−2·3765E−01	−1·8864E−01	−2·6406E−01	−2·8296E−01	−2·3765E−01	−1·8864E−01	−2·6406E−01
1·0E−02	−7·3054E−01	−6·1360E−01	−4·8705E−01	−6·8176E−01	−7·3056E−01	−6·1358E−01	−4·8704E−01	−6·8176E−01
	−2·8298E−01	−2·3768E−01	−1·8866E−01	−2·6408E−01	−2·8299E−01	−2·3768E−01	−1·8866E−01	−2·6408E−01
1·0E+00	−7·2987E−01	−6·1701E−01	−4·8868E−01	−6·8306E−01	−7·3131E−01	−6·1514E−01	−4·8759E−01	−6·8298E−01
	−2·8488E−01	−2·4083E−01	−1·9074E−01	−2·6661E−01	−2·8544E−01	−2·4010E−01	−1·9032E−01	−2·6658E−01
1·0E+01	−7·3196E−01	−6·4309E−01	−5·0204E−01	−6·9305E−01	−7·3772E−01	−6·2648E−01	−4·9217E−01	−6·9205E−01
	−3·0341E−01	−2·6657E−01	−2·0811E−01	−2·8728E−01	−3·0580E−01	−2·5969E−01	−2·0402E−01	−2·8687E−01
1·0E+02	−8·0983E−01	−8·0530E−01	−6·0367E−01	−7·7792E−01	−7·9000E−01	−6·9116E−01	−5·2806E−01	−7·5677E−01
	−4·7921E−01	−4·7653E−01	−3·5722E−01	−4·6032E−01	−4·6748E−01	−4·0899E−01	−3·1248E−01	−4·4781E−01
1·0E+03	−3·4617E+00	1·0975E+01	5·0916E+00	−7·6041E+00	−1·6252E+00	−1·5205E+00	−1·1027E+00	−2·2044E+00
	−6·4982E+00	2·0602E+01	9·5580E+00	−1·4274E+01	−3·0507E+00	−2·8543E+00	−2·0700E+00	−4·1381E+00
1·0E+04	1·5251E−01	1·2470E−01	8·1835E−02	1·2571E−01	2·0922E−01	1·9595E−01	1·3830E−01	1·6558E−01
	1·9203E+00	1·5701E+00	1·0304E+00	1·5828E+00	2·6343E+00	2·4672E+00	1·7414E+00	2·0848E+00
1·0E+05	1·5947E−02	1·4676E−02	9·6072E−03	1·4124E−02	1·8505E−02	1·7933E−02	1·2298E−02	1·6468E−02
	1·7661E+00	1·6253E+00	1·0640E+00	1·5642E+00	2·0494E+00	1·9860E+00	1·3620E+00	1·8238E+00
1·0E+06	1·7635E−03	1·6978E−03	1·1173E−03	1·6415E−03	1·9010E−03	1·8726E−03	1·2655E−03	1·7886E−03
	1·8571E+00	1·7879E+00	1·1766E+00	1·7286E+00	2·0018E+00	1·9720E+00	1·3326E+00	1·8835E+00
1·0E+07	1·8712E−04	1·8387E−04	1·2169E−04	1·8015E−04	1·9406E−04	1·9269E−04	1·2928E−04	1·8829E−04
	1·9272E+00	1·8938E+00	1·2534E+00	1·8554E+00	1·9987E+00	1·9846E+00	1·3316E+00	1·9393E+00
1·0E+08	1·9272E−05	1·9116E−05	1·2697E−05	1·8911E−05	1·9609E−05	1·9544E−05	1·3068E−05	1·9326E−05
	1·9648E+00	1·9489E+00	1·2945E+00	1·9281E+00	1·9991E+00	1·9925E+00	1·3324E+00	1·9704E+00
1·0E+09	1·9545E−06	1·9472E−06	1·2958E−06	1·9369E−06	1·9705E−06	1·9675E−06	1·3135E−06	1·9570E−06
	1·9834E+00	1·9759E+00	1·3149E+00	1·9654E+00	1·9996E+00	1·9965E+00	1·3329E+00	1·9859E+00

Table 6. Convective heat and mass (the upper value in each pair) transport for mercury when $\tau_1 = 0{\cdot}81$.

	$R_s = 1{\cdot}0E+03$				$R_s = 1{\cdot}0E+04$			
Q	Rolls	Squares	Lim. Rect.	Hexagons	Rolls	Squares	Lim. Rect.	Hexagons
1·0E−04	2·9295E+02	2·2650E−02	1·9530E+02	1·3514E−02	−5·2434E+00	2·5457E−01	−3·4956E+00	1·4726E−01
	3·6367E+02	2·8118E−02	2·4244E+02	1·6776E−02	−4·4734E+00	2·1718E−01	−2·9823E+00	1·2563E−01
1·0E−02	2·8492E+02	2·2653E−02	1·8995E+02	1·3516E−02	−5·2437E+00	2·5461E−01	−3·4958E+00	1·4728E−01
	3·5376E+02	2·8126E−02	2·3584E+02	1·6781E−02	−4·4737E+00	2·1722E−01	−2·9825E+00	1·2565E−01
1·0E+00	7·7001E+01	2·2983E−02	5·1334E+01	1·3686E−02	−5·2699E+00	2·5858E−01	−3·5133E+00	1·4925E−01
	9·7062E+01	2·8970E−02	6·4708E+01	1·7251E−02	−4·5061E+00	2·2110E−01	−3·0040E+00	1·2762E−01
1·0E+01	1·1046E+01	2·4929E−02	7·3641E+00	1·4726E−02	−5·4944E+00	2·8174E−01	−3·6630E+00	1·6117E−01
	1·5637E+01	3·5290E−02	1·0425E+01	2·0846E−02	−4·7832E+00	2·4527E−01	−3·1888E+00	1·4031E−01
1·0E+02	1·5191E+00	2·9424E−02	1·0128E+00	1·7887E−02	−7·9854E+00	3·3059E−01	−5·3236E+00	1·9521E−01
	3·8755E+00	7·5065E−02	2·5837E+00	4·5631E−02	−7·8585E+00	3·2534E−01	−5·2390E+00	1·9211E−01
1·0E+03	2·0936E−01	2·9943E−02	1·3958E−01	2·0111E−02	3·4894E+00	3·2565E−01	2·3263E+00	2·1451E−01
	2·2585E+00	3·2300E−01	1·5056E+00	2·1695E−01	6·3079E+00	5·8869E−01	4·2053E+00	3·8777E−01
1·0E+04	2·5576E−02	1·4415E−02	1·7051E−02	1·1234E−02	2·6890E−01	1·4884E−01	1·7927E−01	1·1538E−01
	2·0316E+00	1·1450E+00	1·3544E+00	8·9230E−01	2·3320E+00	1·2908E+00	1·5547E+00	1·0006E+00
1·0E+05	2·8284E−03	2·5035E−03	1·8856E−03	2·2535E−03	2·8438E−02	2·5161E−02	1·8958E−02	2·2641E−02
	2·0035E+00	1·7733E+00	1·3357E+00	1·5962E+00	2·0351E+00	1·8006E+00	1·3567E+00	1·6203E+00
1·0E+06	2·9653E−04	2·8738E−04	1·9768E−04	2·7537E−04	2·9669E−03	2·8754E−03	1·9780E−03	2·7552E−03
	2·0004E+00	1·9386E+00	1·3336E+00	1·8577E+00	2·0037E+00	1·9418E+00	1·3358E+00	1·8607E+00
1·0E+07	3·0309E−05	2·9986E−05	2·0206E−05	2·9437E−05	3·0310E−04	2·9988E−04	2·0207E−04	2·9438E−04
	2·0000E+00	1·9788E+00	1·3334E+00	1·9425E+00	2·0004E+00	1·9791E+00	1·3336E+00	1·9428E+00
1·0E+08	3·0617E−06	3·0485E−06	2·0411E−06	3·0231E−06	3·0617E−05	3·0485E−05	2·0411E−05	3·0231E−05
	2·0000E+00	1·9914E+00	1·3333E+00	1·9748E+00	2·0000E+00	1·9914E+00	1·3334E+00	1·9748E+00
1·0E+09	3·0761E−07	3·0703E−07	2·0507E−07	3·0585E−07	3·0761E−06	3·0703E−06	2·0507E−06	3·0585E−06
	2·0000E+00	1·9962E+00	1·3333E+00	1·9886E+00	2·0000E+00	1·9962E+00	1·3333E+00	1·9886E+00

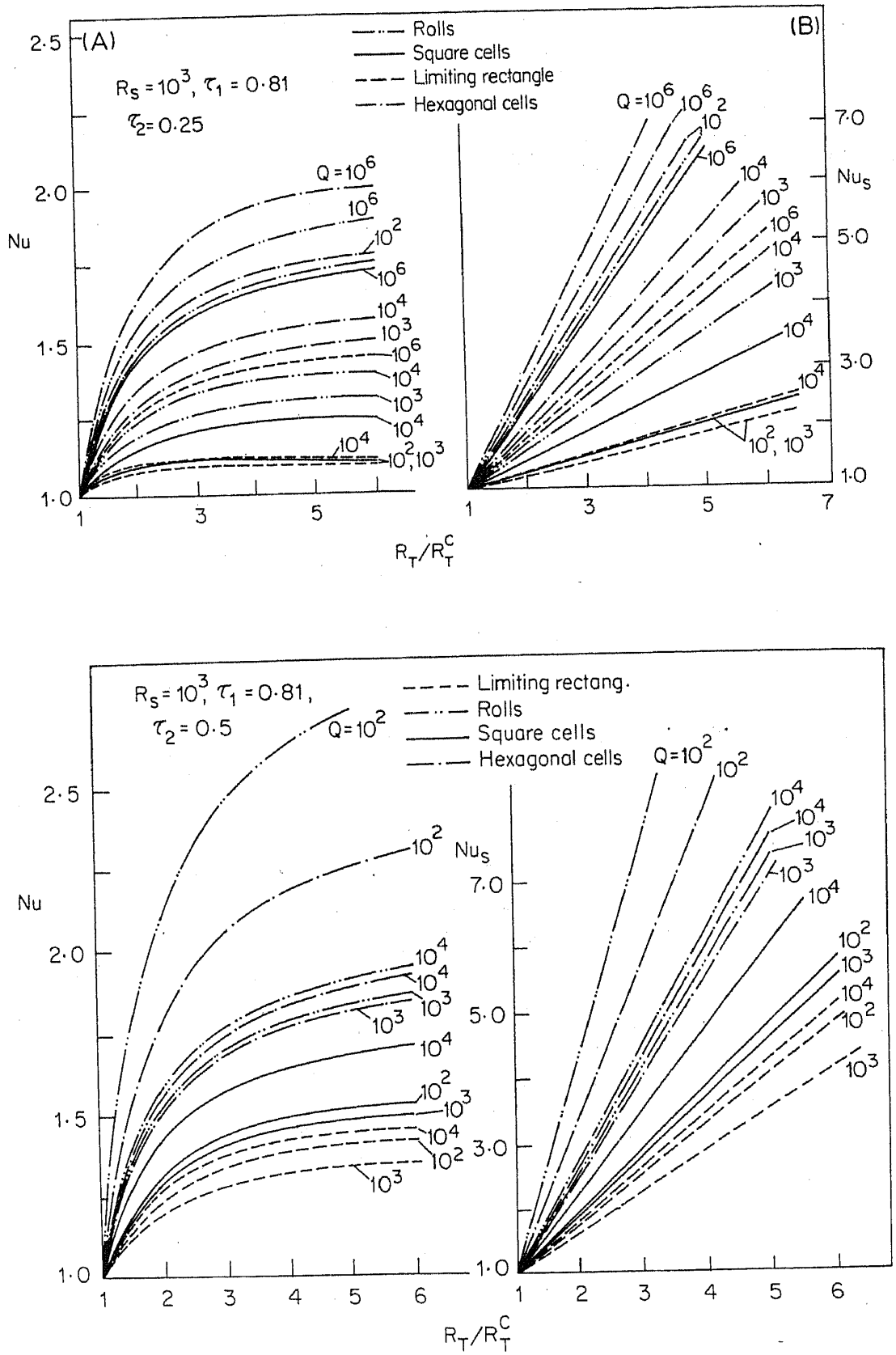

Figure 10. Nu and Nu_s for two and three-dimensional convection for different values of Q.

Figure 10 clearly depicts the preferred cell pattern for different values of Q, R_s ($= 10^3$), τ_2 ($= 0{\cdot}25, 0{\cdot}5$) for a fixed value of $\tau_1 = 0{\cdot}81$. From these figures we note that $\mathrm{Nu}_s > \mathrm{Nu}$ always. The oscillatory nature of heat and mass transport may be due to the existence of finite amplitude overstable motion. Figure 11 is a plot of convective heat and mass transport against the values of l/m and it is found that there is a sudden increase in heat and mass transport for values of $l/m < 0{\cdot}6$ and remain uniform for values of $l/m \geqslant 0{\cdot}6$.

Finally, we claim that it is possible to prevent convection altogether by a proper choice of the parameters. One such case is considered and the results are shown in table 7 for rolls. From this table it is clear that for $Q = 7{\cdot}317 \times 10^4$ convection can be prevented altogether. The velocity and magnetic stream functions are drawn in figures 12a and 12b and we see that the effect of magnetic field is to contract the cells.

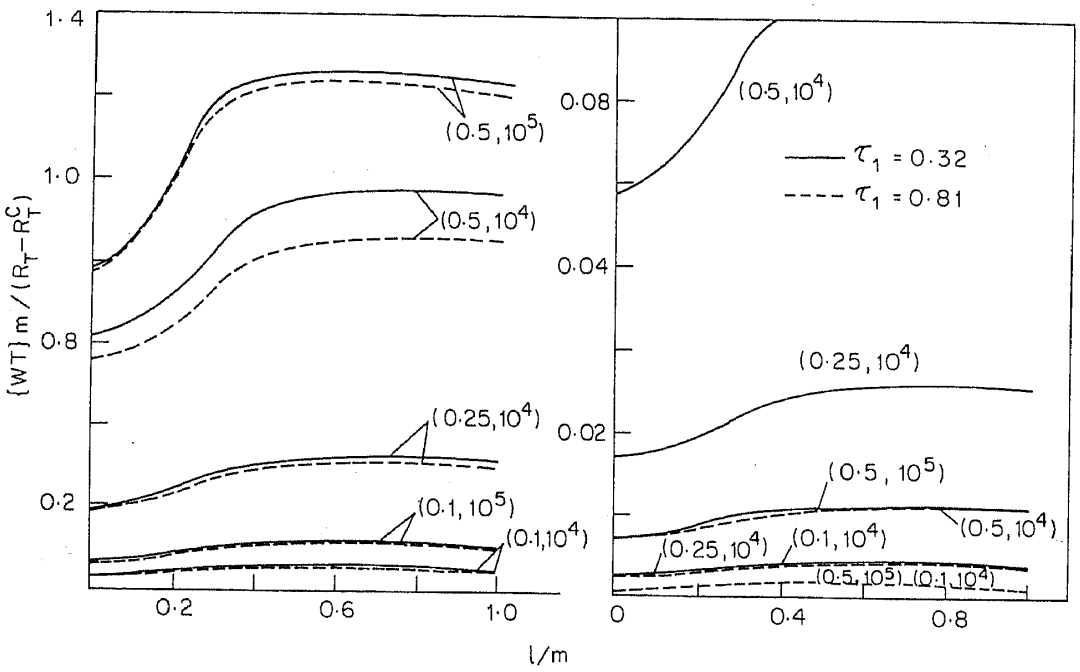

Figure 11. Heat and mass transport for the general rectangle at several pairs of values of (τ_2, Q) for $R_s = 10^3$.

Table 7. Nusselt number for different values of Q for $R_s = 1000$, $\tau_1 = 0{\cdot}32$, $\tau_2 = 0{\cdot}25$ and $R_T = 8{\cdot}0\mathrm{E}+05$.

Q	Nu
4·0E + 02	2·894
8·0E + 02	1·748
1·0E + 03	1·653
2·0E + 03	1·518
4·0E + 03	1·475
8·0E + 03	1·460
1·0E + 04	1·455
2·0E + 04	1·416
4·0E + 04	1·288
7·317E + 04	1·000

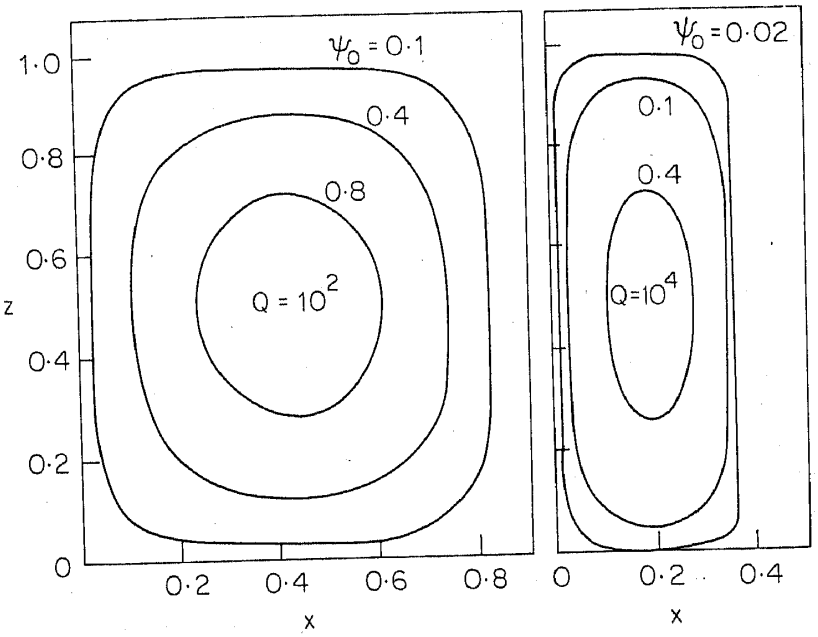

Figure 12a. Velocity stream function for $R_s = 10^3$, $\tau_1 = 0{\cdot}32$.

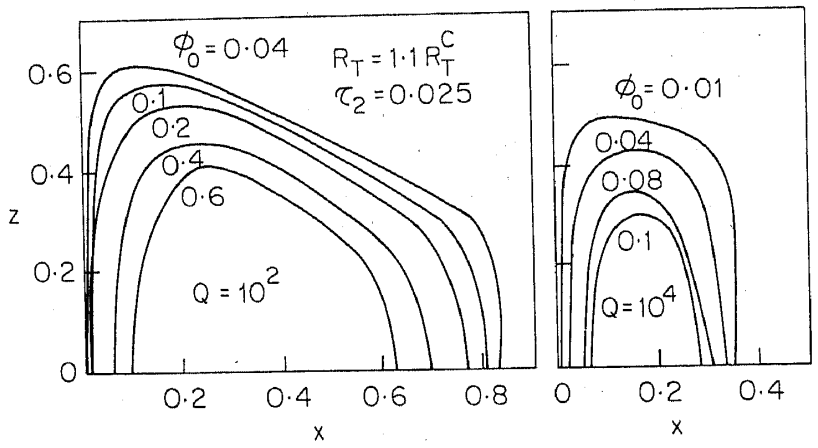

Figure 12b. Magnetic stream function for $R_c = 10^3$ and $\tau_1 = 0{\cdot}32$.

9. Further results

9.1 *Double-diffusive magnetoconvection caused by coupled molecular diffusion*

The systematic study of the effect of cross-diffusion on double-diffusive magneto-convection constitutes a comparatively recent development (Rudraiah *et al* 1986b) in theoretical fluid mechanics with applications in astrophysics and geophysics. In ordinary viscous flow, the linear stability of double-diffusive convection with two cross-diffusion flux terms has been investigated by McDougall (1983). He showed, with a sufficiently large coupled diffusion effect, that either the 'finger' or diffusive 'modes of double diffusive convection may occur even when both components make the fluids'

density gradient statically stable. Kerr (1984) studied the nonlinear double-diffusive convection by including two cross-diffusion flux terms subject to a finite-amplitude perturbation using minimal representation of modal analysis. He showed that finite amplitude double-diffusive convection can occur in a fluid where both property gradients are stabilizing for relatively small and negative values of the cross-diffusion coefficients. Recently, Rudraiah *et al* (1986b) have extended the linear and nonlinear stability analysis of double-diffusive magnetoconvection (Rudraiah and Shivakumara 1984, 1986a) by including two cross-diffusion flux terms. To discuss the stability Rudraiah *et al* (1986b) used the usual stress-free boundary conditions. The stability analysis for this problem is reminiscent of that described in the previous sections.

9.2 *Double-diffusive magnetoconvection in liquid mixtures with "fast" chemical reaction*

The problem of reactive liquid mixtures evolved around the same time as the cross-diffusion problem mentioned in §9.1. The hydrodynamic convective instability of double diffusive liquids with chemical reaction was studied by Gitterman and Steinberg (1983). They introduced two essential approximations to isolate the influence of a chemical reaction on the hydrodynamic stability and to obtain an analytical solution. First, they neglect the effect of thermal diffusion (Soret effect) since its influence on the stability is usually much smaller than that of a chemical reaction. Second, they assume the approximation of "fast" chemical reaction. This means that the chemical reaction is fast compared with the diffusion rate. They obtained, based on the above two approximations, numerical estimates for both stationary and oscillatory instabilities. However, their work is silent about the possibility of subcritical instability.

Rudraiah and his co-workers are presently engaged in studying the hydromagnetic convective instability of double diffusive liquids with fast chemical reaction. The results of this problem have potential applications in astrophysics and geophysics in addition to technological applications, but the study of this problem lies beyond the scope of this review.

9.3 *Rotation*

Rotation is known to have profound effects in fluid mechanics. Geophysical flows are strongly influenced by the earth's rotation ($\Omega \approx 10^{-4}\ \mathrm{sec}^{-1}$). Similarly astrophysical flows in the sun ($\Omega \approx 10^{-6}\ \mathrm{sec}^{-1}$), and in crab pulsar ($\Omega \approx 10^{2}\ \mathrm{sec}^{-1}$) are also influenced by the Coriolis force. The double-diffusive convective flows are stabilized or destabilized by the introduction of rotation. These effects on double-diffusive convection in the presence of magnetic field are described by Rudraiah *et al* (1986a). Since turbulence is created by instability it is strongly affected by the combined system of rotation and magnetic field. Recently, Rudraiah and Shivakumara (1986c) have studied the combined effects of rotation and magnetic field on double-diffusive magnetoconvection. They have shown that the combined effect of rotation and magnetic field with bottom-heavy solute gradient renders the system unstable under certain conditions. The detailed linear and nonlinear study of this problem has been made recently by Shivakumara (1985) and it is beyond the scope of this review.

9.4 *Pattern selection*

The double-diffusive magnetoconvection discussed in this review provides one of the best studied examples of nonlinear pattern selection. Although the critical wavenumber

depends purely on the magnetic field, both Q and R_s influence the pattern selection. For small temperature differences, measured by R_T, heat and mass are transported by molecular conduction. As R_T is increased the conduction state loses stability and the effect of Q and R_s is to inhibit it. At $R_T = R_T^{(c)}$, the point of neutral stability, the linear stability problem admits several different planforms like rolls, square and hexagons. For supercritical values of R_T the amplitude of each planform grows exponentially until the nonlinear effects become important and the effect of magnetic field is to suppress the amplitude. The nonlinear terms are responsible for selecting one of the planforms depending on symmetry of the problem.

In the case of a single component Boussinesq fluid in the absence of magnetic field if the boundary conditions are the same at the top and bottom surfaces and the basic temperature gradient is uniform Schlüter *et al* (1965) predicted that in a large aspect ratio container rolls are the preferred cell pattern. However, in the case of double-diffusive magnetoconvection Rudraiah and Shivakumara (1986b) (see § 7.2) have shown using perturbation technique that the hexagons are the preferred cell pattern for certain ranges of the parameters involved. Although this perturbation method yielded many interesting and valuable results it suffers from two disadvantages; First, it does not take full advantage of various symmetries of the problem. Second, perturbation expansions carried out to some order and the higher order terms are neglected without adequate justification. The basic question here is, what order expansion must be taken if the addition of higher order terms is not to change any qualitative aspects of the dynamics. Results of this kind are called structural stability results. The proof of structural stability is almost impossible. Recently, Golubitsky *et al* (1985) studied the preferred cell pattern in the Rayleigh Bénard convection in the absence of magnetic field by means of group theory. It is, therefore, advantageous to study the pattern selection in a double-diffusive magnetoconvection by means of either singularity theory or group theory. Work in this direction is in progress.

References

Baines P G and Gill A E 1969 *J. Fluid Mech.* **37** 289
Busse F H 1975 *J. Fluid Mech.* **71** 193
Chandrasekhar S 1961 *Hydrodynamic and hydromagnetic stability* (Oxford: Clarendon Press)
Chen C F and Johnson D H 1984 *J. Fluid Mech.* **138** 405
Da Costa L N, Knobloch E and Weiss N O 1981 *J. Fluid Mech.* **109** 25
Friedman B 1956 *Principles and techniques of applied mathematics* (New York: John Wiley)
Gitterman M and Steinberg V 1983 *Phys. Fluids* 26(2) 393
Golubitsky M, Swift J W and Knobloch E 1985 (Private communication)
Griffiths R W 1979a *Deep Sea Res.* **26** 383
Griffiths R W 1979b *Int. J. Heat Mass Transfer* **22** 1687
Griffiths R W 1979c *J. Fluid Mech.* **92** 659
Griffiths R W and Ruddick B R 1980 *J. Fluid Mech.* **99** 85
Griffiths R W 1981 *J. Fluid Mech.* **102** 221
Huppert H E and Moore D R 1976 *J. Fluid Mech.* **78** 821
Huppert H E and Turner J S 1981 *J. Fluid Mech.* **106** 299
Kerr R C 1984 Woods Hole Oceanographic Institution, Report No. 84-44, 218
Knobloch E and Weiss N O 1983 *Physica* **D9** 379
Lortz D 1965 *J. Fluid Mech.* **23** 113
Malkus W V R and Veronis G 1958 *J. Fluid Mech.* **4** 225
Mc Dougall T J 1983 *J. Fluid Mech.* **126** 374

Narayanan R 1983 *J. Engg. Mathematics* **11** 223
Narayanan R 1984 *Int. J. Engg. Sci.* **22** 927
Nield D A 1968 *Water Resources Res.* **4** 553
Pearlstein A J 1981 *J. Fluid. Mech.* **103** 389
Peckover R S and Weiss N O 1978 *Mon. Not. R. Astr. Soc.* **182** 189
Proctor M R E and Weiss N O 1982 *Magnetoconvection, Rep. Prog. Phys.* **45** 1317
Rayleigh, Lord 1916 *Philos. Mag.* **32** 529
Rudraiah N 1981 *Publ. Astron. Soc. Jpn* **33** 721
Rudraiah N, Srimani P K and Fiedrich R 1982a *Int. J. Heat Mass Transfer* **25** 715
Rudraiah N, Srimani P K and Friedrich R 1982b *7th Int. Heat Transfer Conf.*, Munich
Rudraiah N and Shivakumara I S 1984 *Int. J. Heat Mass Transfer* **27** 1825
Rudraiah N, Kumudini V and Unno W 1985a *Publ. Astron. Soc. Jpn* **37** 183
Rudraiah N, Kumudini V and Unno W 1985b *Publ. Astron. Soc. Jpn* **37** 207
Rudraiah N, Shivakumara I S and Friedrich R 1986a *Int. J. Heat Mass Transfer* (in press)
Rudraiah N and Shivakumara I S 1986a *Z. Angew. Math. Phys.* (submitted for publication)
Rudraiah N and Shivakumara I S 1986b *Publ. Astron. Soc. Jpn* (submitted for publication)
Rudraiah N and Shivakumara I S 1986c (under preparation)
Rudraiah N, Siddheshwar P G and Shivakumara I S 1986b (under preparation)
Schluter A, Lortz D and Busse F H 1965 *J. Fluid Mech.* **23** 129
Shivakumara I S, Rudraiah N and Narayanan R 1985 *Int. Commun. Heat Mass Transfer* **12** 299
Shivakumara I S 1985 *Convection of two- and three-component systems in a horizontal layer*, Ph.D. thesis, Bangalore University
Stommel H, Arons A B and Blanchard D 1956 *Deep Sea Res.* **3** 152
Taunton J W, Lightfoot E N and Green T 1972 *Phys. Fluids* **15** 748
Turner J S 1974 *Annu. Rev. Fluid Mech.* **6** 37
Turner J S 1979 *Buoyancy effects in fluids* (Cambridge: University Press)
Turner J S 1981 *Proc. 2nd Int. Conf. on turbulence in the Ocean* (ed.) J D Woods (Berlin: Springer–Verlag)
Tyvand P A 1980 *Water Resources Res.* **16** 325
Veronis G 1959 *J. Fluid Mech.* **5** 401
Veronis G 1966 *J. Fluid Mech.* **24** 545
Wankat P C and Schowalter W R 1970 *Phys. Fluids* **13** 2418
Weiss N O 1981a *J. Fluid Mech.* **108** 247, 273